MATERIALS CHEMISTRY
FRONTIERS

REVIEW

View Article Online
View Journal | View Issue

Cite this: *Mater. Chem. Front.*, 2020, **4**, 369

Carbon-based dots for electrochemiluminescence sensing

Ying Chen, Yue Cao, Cheng Ma* and Jun-Jie Zhu*

Carbon materials based quantum dots, mainly including carbon and graphene dots, with wonderful optical, electrical and chemical properties have greatly boosted the development of advanced sensors and analytical chemistry. Electrochemiluminescence (ECL) sensors based on carbon and graphene dots have shown promising potential and rapid developments in recent decades and have also attained great achievements. Deep insight into the applications of carbon and graphene dots in ECL sensing platforms will benefit the design of advanced sensors in the future. In this review, we aim to give a brief overview of carbon and graphene dots with versatile roles in the fabrication of ECL sensors. A general description of the basic ECL mechanisms, main synthesis routes of carbon and graphene dots, and a series of sensing approaches for the detection of targets including metal ions, small molecules, proteins, DNA and cells will be presented. In addition, recent developments of ECL sensors made of carbon-based dots, relevant signal amplification methodologies and an outlook for the construction of highly sensitive ECL sensors based on various carbon-based dots are also discussed.

Received 12th September 2019,
Accepted 15th October 2019

DOI: 10.1039/c9qm00572b

rsc.li/frontiers-materials

1. Introduction

Nanomaterials, the building blocks of nanotechnology, exhibit wonderful optical, electrical and chemical properties, making them very attractive to scientists and researchers in various areas.[1–5] Among all kinds of nanomaterials, carbon based nanomaterials have gained enormous attention, especially carbon-based quantum dot materials.[6–9] Due to their excellent performance in many different ways, attention towards the application of carbon-based dots in the area of electrochemiluminescence (ECL) sensing has been rapidly increasing in recent years. ECL is a process involving light emission by species generated at electrodes when they undergo highly energetic electron-transfer reactions and form excited states.[10] ECL technology is the marriage of electrochemistry and spectroscopy combining the advantages of both, such as the absence of a light source, accurate control over the potential, position and time of the light-emitting process, versatile luminophores, fast response speed, simple operation process and low-cost devices.[11–13] The introduction of carbon-based dots into ECL sensors has highly advanced the sensitivity and diversity of the sensing area. Carbon-based dots have plenty advantages such as simple synthesis, low cost, and most of all, their excellent physical and chemical properties.[14,15] Besides, carbon-based dots are water-soluble, biocompatible, environmentally friendly and

State Key Laboratory of Analytical Chemistry for Life Science, School of Chemistry and Chemical Engineering, Nanjing University, Nanjing, Jiangsu, 210023, China. E-mail: chengma@nju.edu.cn, jjzhu@nju.edu.cn

Ying Chen

Ying Chen received her BS degree from Nanjing University in 2013. In 2019 she completed her PhD research in Prof. Jun-Jie Zhu's group at the School of Chemistry and Chemical Engineering, Nanjing University, China. Her research focuses on multifunctional nanomaterials and their applications in electrochemiluminescence sensing and imaging.

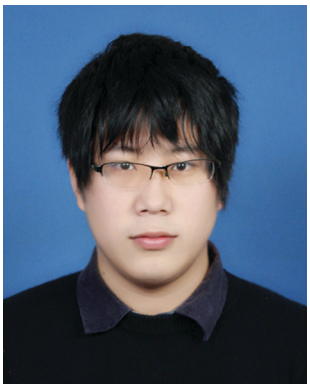

Yue Cao

Yue Cao obtained both his BSc and MSc in chemistry from Yangzhou University. He is currently a PhD candidate with Prof. Jun-Jie Zhu at the School of Chemistry and Chemical Engineering, Nanjing University. His research involves development and functionalization of novel nanomaterials and their applications in the electrochemiluminescence domain.

less toxic, with carboxylic acid moieties on the surface making them easy to functionalize with various agents.[16] The sources to synthesize carbon-based QDs are abundant including graphite, polymers, even hair fibers and coffee grounds.[17–20]

Generally speaking, carbon dots (CDs) and graphene dots (GDs) are considered as two major kinds of carbon-based dots due to their distinct morphologies and structures.[21] CDs are classic zero-dimensional (0D) materials with diameters less than 10 nm.[22,23] They may be amorphous or nanocrystalline with sp^2 carbon clusters.[22] GDs are similar to graphene nanosheets but have a lateral dimension of less than 100 nm.[24] Moreover, GDs have clear graphene structures in the dots, and high crystallinity regardless of the size of the dots.[14,25] CDs and GDs are considered as excellent candidates for ECL sensor materials, due to the following advantages. First, their unique electrochemical properties, such as great stability and huge specific surface area, not only make them novel ECL luminophores but also superior electrode materials.[26] Second, their excellent electrochemical properties with good electron mobility facilitate charge transfer and boost the electrochemical activity.[25] Third, their chemical and electrical properties are highly tunable with various sizes and surface states.[27] Last but not least, there are abundant defects and chemical groups on their surfaces giving flexibility for various kinds of functionalization.[22] Thus, CDs and GDs can play diverse roles in ECL sensing application such as a new class of nano-emitters, electrode modification materials, reaction catalysts and so on, promoting great developments in advanced ECL sensors. They can enhance the efficiency of both recognition part and transducer part, which are the two major components of ECL biosensors, showing impressive strength in the area of ECL sensing.

Here in this review, we aim to give a succinct overview of the development of carbon-based dots applied in ECL sensing. For better understanding, basic ECL mechanisms and common sensing strategies are introduced. A general introduction to the main synthesis methods for carbon and graphene dots is presented. Particular emphasis on the applications of carbon and graphene dots in different kinds of ECL sensors is made. A brief outlook on the potential development directions of future carbon nanomaterials-based ECL sensors is provided in the final part.

2. The bases of electrochemiluminescence sensing

ECL is a powerful and convenient technique for sensing applications. Since the pioneering studies of Hercules and Bard in the 1960s,[28,29] investigations on ECL mechanisms and designs of ECL sensors have become hotspots in the field of analytical chemistry. Generally, an ECL process can be produced through two dominant pathways, namely, the annihilation pathway and the coreactant pathway.[10] In a traditional annihilation pathway, oxidized and reduced species are both electrogenerated near the electrode surface when potential pulsing or cycling is applied onto an electrode. Then the oxidized species and reduced species collide in an annihilation process to form excited species which will further emit ECL light. The potential applied onto the electrode should be sufficient for the formation of both oxidized and reduced species. And ECL species need to be chemically stable and should maintain charged states long enough.[30] In contrast, for the coreactant pathway where coreactants and ECL active species coexist at the same time, it is possible to generate ECL emission only with a single direction potential sweep. A coreactant is the substance that can undergo an intermediate reaction with ECL luminophores to generate excited species upon electrooxidation or electroreduction.[11] In comparison with the annihilation pathway, the coreactant pathway has better radical ion stability in the aqueous phase, stronger ECL intensity and extensive universality,[31] making it much more popular in practical applications. A well-studied example of the coreactant pathway is the ECL system of tris(bipyridine)-ruthenium(II) ($Ru(bpy)_3^{2+}$) with tripropylamine (TPrA) as the coreactant.[12] This system made a

Cheng Ma

Cheng Ma received his BS degree in Chemistry in 2011 and MS degree in Analytical Chemistry in 2014, both from Hunan University. In 2018, he completed his PhD degree in Analytical Chemistry in Prof. Jun-Jie Zhu's group at the School of Chemistry and Chemical Engineering, Nanjing University, China. Currently, he is an associate research fellow in Jun-Jie Zhu's group at Nanjing University. His main research passion and strength focus on electrochemiluminescence microscopy and spectra at single-nanoparticle and single-cell levels.

Jun-Jie Zhu

Jun-Jie Zhu received his BS (1984) and PhD (1993) degrees from the Department of Chemistry, Nanjing University, China. Then, he began his academic career at the School of Chemistry and Chemical Engineering, Nanjing University. He entered Bar-Ilan University, Israel, as a postdoctoral researcher from 1998 to 1999. Since 2001, he has been a full professor at the School of Chemistry and Chemical Engineering, Nanjing University. His main research activities focus on preparation and application of functional nanomaterials, and fabrication of electrochemical and electrochemiluminescence biosensors.

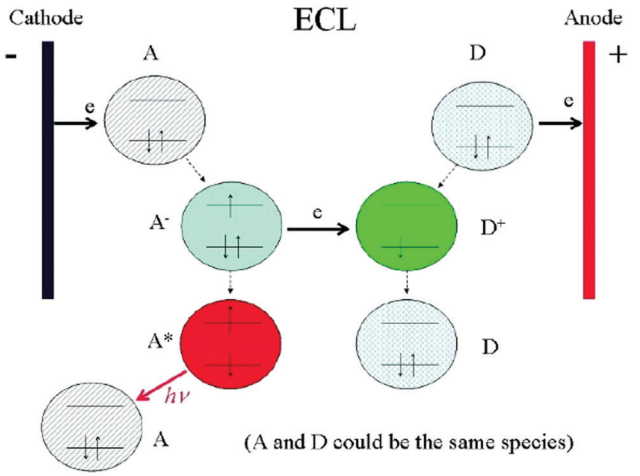

Fig. 1 Schematic diagrams showing the general principles of ECL. Reprinted with permission from ref. 33. Copyright (2007) Elsevier.

vital contribution in bringing ECL biosensors into clinical applications.[32]

In spite of different ECL pathways, there are generally four steps in most of the ECL processes, namely, redox reactions at electrodes, homogeneous chemical reactions, excited state species formation and light emission (Fig. 1).[33] Theoretically, any molecules that can interfere (inhibit or promote) the above steps will change the final ECL emission and thus can be quantitatively detected. Accordingly, we classify the ECL sensing strategies into five main types. The most classic way is the direct usage of an ECL emitter as a signal label. Another common route is to use steric hindrance or impedance effect caused by bio-recognition reactions. The interaction between analytes and ECL species such as ECL luminophores, ECL luminophore radicals or excited ECL species is also a convenient way to cause an ECL signal change. The fourth strategy relies on the interaction between analytes and coreactant species, which is suitable for coreactant ECL systems. The most elaborate route aims at ECL light emission, mainly achieved by an emerging technology called ECL resonance energy transfer (ECL-RET). RET is a non-radiative process whereby energy transfers through long-range dipole–dipole interactions from an excited-state donor to a proximal ground-state acceptor.[34] In this case, the ECL donor gives high emission intensity, while the analyte-related acceptor is designed to change the ECL emission intensity through RET. Thanks to the intrinsic sensitivity of the ECL-RET method with the donor–acceptor distance on the nanoscale, and the various possibilities of nanomaterials serving as ECL donors or acceptors, this novel route gives nanomaterials more space to show their strength in ECL sensing applications.

3. Synthesis and modification of carbon-based dots

3.1. Synthesis methods for carbon-based dots

Up to now, various kinds of synthesis methods for carbon-based dots have been reported. Here, we divide them into two major categories, *i.e.* the top-down synthesis methods and the bottom-up synthesis methods. The top-down synthesis methods usually involve the extraction of carbon nanoparticles from a larger carbon skeleton, mainly including chemical ablation, laser ablation and electrochemical synthesis.[35–38] The bottom-up synthesis methods involve direct formation for carbon nanoparticles, mainly including hydrothermal treatment, precursor pyrolysis/carbonization and microwave irradiation.[35,36] Different synthesis methods can lead to different kinds of physical and chemical properties and performances, which can be applied to different applications.

3.1.1. Top-down synthesis. As mentioned before, carbon-based dots synthesized by the top-down methods are generated from relatively large carbon skeletons such as carbon powders, carbon fibers, graphene and even graphite rods. Thus, the top-down methods have abundant resources and can realize the diversification of size and surface states for carbon-based dots. Chemical ablation involves the oxidation of carbon skeletons by oxidative reagents. It usually results in abundant oxygen-containing functional groups such as OH and COOH, bringing excellent hydrophilicity and functionalization to the carbon-based dots.[36,39] Ganesh prepared green color emitting GDs from graphene oxide using an acid reflux reaction.[40] This kind of GD showed a stable and uniform structure, and had plenty of surface functional moieties such as epoxide, hydroxyl and carboxyl groups, which were easily immobilized with biomolecules.[40] Pang *et al.* reported the synthesis of a series of CDs from carbon fibers by varying the reaction temperature, time, and concentration of nitric acid. The size, the degree of surface oxidation and the fluorescence colors of CDs could be controlled, providing new insight into the synthesis of multicolor CDs with respect to both experiments and mechanisms. The electrochemical synthesis method was first reported by Zhou *et al.*[41] They used multi-walled carbon nanotubes as the working electrode and applied a cyclic potential in a degassed acetonitrile solution with 0.1 M tetrabutylammonium perchlorate.[41] CDs are formed from the peeled nanotubes when the colorless solution turned dark brown.[41] Ananthanarayanan *et al.* reported GDs synthesized *via* a "green" electrochemical strategy, which were electrochemically exfoliated from graphene grown by the chemical vapor deposition method (Fig. 2).[42] Different protocols for electrochemical exfoliation were attempted, and turned out that a high yield of GDs with preserved graphene structure could be obtained by applying a constant 5 V voltage for 100 s.[42] The obtained GD dispersion showed a blue fluorescence under UV light, which could be selectively quenched by Fe^{3+} ions.[42]

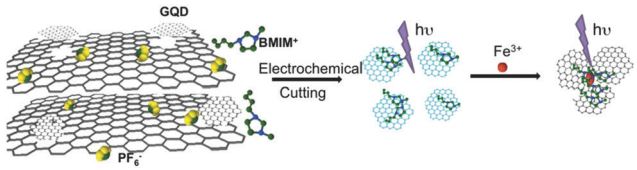

Fig. 2 Schematic illustration of GD synthesis from 3D graphene and the mechanism of Fe^{3+} detection. Reprinted with permission from ref. 42. Copyright (2014) Wiley-VCH Verlag GmbH & Co. KGaA, Weinheim.

To prepare CDs with tunable surface states and excellent ECL properties on a large scale, a mechanochemical method with ball milling was conducted for the preparation of CDs with multiple surface states.[43] The as-prepared CDs showed dual-potential ECL emission and dual-peak fluorescence emission, where the first peak is unrelated to the excitation wavelength but the second is related. However, the top-down approaches usually use a nonselective cutting process, making it hard to gain precise control over the size and properties of the carbon-based dot products.

3.1.2. Botton-up synthesis. In the bottom-up synthesis process, the precursors act as seeds and grow into carbon-based dots under various reaction conditions, commonly by heating or microwave.[44] Numerous molecules containing the carbon element such as glucose,[45] L-glutamic acid[46] and arginine/ethylenediamine[47] can be used to prepare carbon-based dots. More importantly, the bottom-up methods often have good control over the size and properties of the carbon-based dot products. The hydrothermal method is an efficient way to obtain carbon-based dots with high quality, commonly through polymerization and carbonization reactions.[36] To obtain geometrically well-defined GDs with a solution-processable and scalable approach, unsubstituted hexa-*peri*-hexabenzocoronene was used as a precursor by pyrolysis and the morphology of the GDs can be regulated by the pyrolysis temperature.[48] Subsequently, citric acid and glutathione were considered as two precursors for the synthesis of GDs with high fluorescence quantum yield due to the introduction of glutathione.[49] Similarly, Lin *et al.* developed a one-step pyrolysis of citric acid and tris(hydroxymethyl)amino-methane for N-doped GDs with a high fluorescence quantum yield of 59.2%.[50] In addition to common precursors, Wu *et al.* discovered that a natural amino acid, L-glutamic acid, can form highly fluorescent N-doped GDs with the assistance of a simple heating mantle device. The as-prepared GDs showed a variety of fluorescence spectra ranging from the visible to the near-infrared fluorescence region, allowing *in vivo* fluorescence imaging with low background signals.[46] High-quality GDs with superior luminescence properties are highly desirable for many applications while current synthetic methods often generated polycrystalline and defect-rich structures, thereby leading to poor optical performance. To address this problem, Wang *et al.* synthesized water-soluble single crystal GDs with well-passivated edge sites by alkali-mediated hydrothermal molecular fusion using a polycyclic aromatic hydrocarbon as the precursor.[51] The proposed method enables large-scale synthesis of single-crystalline GDs with high quantum yield and long-term photostability.

The use of microwaves provides a promising alternative synthetic approach besides pyrolysis procedures. Moreover, microwave processes avoid sophisticated synthesis steps and provide benefits from characteristics like faster rates, milder conditions, and low energy consumption.[47] Nevertheless, these pristine CDs derived from conventional microwave approaches usually suffer from a relatively low quantum yield.[52] Many reports demonstrated that heteroatom-doping by the introduction of amine-group enriched molecules during the microwave pyrolysis can improve the luminescence performance.[47,53] For example, the Liu group developed one-step microwave-assisted pyrolysis of citric acid in the presence of various amine molecules given that the passivation agents of amine groups during the microwave process can improve the fluorescence quantum yield.[53–55] In addition, N-doped CDs could be obtained within three minutes using arginine and ethylenediamine as carbon and nitrogen sources under microwave irradiation.[47] This approach avoided sophisticated equipment and additional surface passivation. More interestingly, low-pressure gel permeation chromatography was employed for the separation of three fractions of N-doped CDs with different sizes and properties. Luo *et al.* used a microwave-assisted solvothermal approach to synthesize N and S co-doped reduced graphene oxide functionalized with GDs, which not only showed high fluorescence but also good electrocatalytic performance for the oxygen reduction reaction.[56] In another approach, 3,4-dihydroxy-L-phenylalanine (levodopa) was used as the carbon resource to synthesize CDs with good crystallinity under mild conditions by a microwave assisted approach.[57] Interestingly, a kind of CD with fluorescence and ultra-long phosphorescence was synthesized using *n*-aminoethyl-trimethoxysilane and phosphoric acid as precursors through a facile microwave-directed method (Fig. 3).[58] These CDs showed a blue fluorescence under UV light irradiation and a long-life green phosphorescence when the UV light was switched off, indicating a dual channel assaying model.

3.2. Modification of carbon-based dots

Due to the large specific surface area, good stability and versatile modification with different kinds of functional groups (for example, hydroxyl, carboxyl and amino groups), along with the strong π–π conjugation and electrostatic adsorption, diverse molecules such as biomolecules (enzyme, antibody, DNA), organic molecules and nanoparticles can be immobilized on carbon-based dots. Thus, carbon-based dots are often modified as electrode surface substrates and signal probes in a variety of sensors.

3.2.1. Modification as electrode substrates. Chen *et al.* used Nafion to modify CDs into an architecture layer as the substrate to further immobilize antibodies, and they found that the good conductivity of CDs could promote electron transfer to

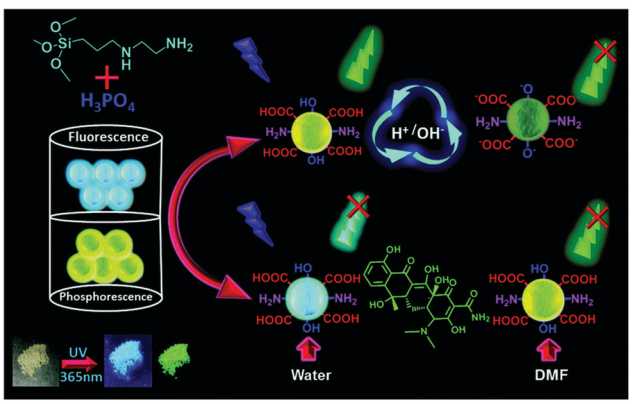

Fig. 3 Schematic of the synthesis of P-CDs and their pH-sensing, and the use of P-CDs for the dual-channel detection of tetracycline. Reprinted with permission from ref. 58. Copyright 2019 Royal Society of Chemistry.

improve the sensitivity of electrochemical response.[59] By modifying CDs into polyamidoamine (PAMAM)–CDs/Au nanocomposites, Gao *et al.* synthesized a new substrate for immobilization of anti-alpha-fetoprotein (anti-AFP), which showed excellent conductivity, stability and biocompatibility (Fig. 4).[60] In another work, nitrogen-doped carbon dots (N-doped CDs) were modified with enzymes as the substrate, which promoted the electron transfer between the enzyme and electrode and enhanced the electrocatalytic activity for glucose determination.[61] Punrat *et al.* reported a polyaniline/GD based electrochemical sensor, in which the GDs were synthesized from citric acid in a bottom-up manner, and were mixed with aniline monomers for electro-polymerization to obtain a polyaniline/GD modified screen-printed carbon electrode, which was then applied in the sensing of Cr ions.[62] As mentioned above, the green color emitting GDs prepared by Ganesh *et al.* had plenty of surface functional moieties such as epoxide, hydroxyl and carboxyl groups, which were further modified with the horseradish peroxidase (HRP) enzyme through amide interactions.[40] This HRP modified GD substrate was applied for hydrogen peroxide (H_2O_2) detection.[40] Dong *et al.* used GDs with abundant hydroxyl and carboxyl groups as the substrate for glassy carbon electrode (GCE) modification, and then attached pralidoxime (PAM), a commonly used antidote for organophosphorus pesticides (OPs), on the GDs by electrostatic adsorption and π–π stacking interactions to detect OP concentration.[63]

3.2.2. Modification as probes. Benefiting from the large specific surface area, easy functionalization and unique luminescent properties, carbon-based dots are also often modified in the probes and used for the amplification of response signals in sensors. Besides, carbon-based dots are very suitable as carriers to adsorb abundant probes such as organic molecules, biomolecules and other nanomaterials due to their superior dispersibility, biocompatibility, and electrostatic adsorption property. In an electrochemical sensor for Cu^{2+} ions, CDs with surface carboxyl and hydroxyl groups were modified with *N*-(2-aminoethyl)-*N*,*N*′,*N*′-tris-(pyridine-2-yl-methyl)ethane-1,2-diamine (AE-TPEA) by amide interactions to achieve Cu^{2+} probes, which were applied in the determination of cerebral Cu^{2+} in rat brain micro-dialysates.[64] In a multifunctional sensor for ascorbic acid (AA), uric acid (UA), dopamine (DA), and acetaminophen (AC), CDs were used to synthesize a Au NPs/carbon dot nanocomposite (Au/C NC) and modified with a thiol functionalized ferrocene derivative (Fc-SH) as probes. And the CDs played a crucial bridge-effect role in immobilizing the probes on graphene sheets using the interaction between CDs and graphene.[65] Hu *et al.* prepared a kind of GD with carboxyl and hydroxyl groups, and modified them as carriers by amide interactions and the hybridization reaction among aminated indicator probe, thiol-tethered probe and target DNA. On the other hand, horseradish peroxidase was immobilized by strong π–π conjugation and electrostatic adsorption of GDs, resulting in an electrochemical enzyme sensor for quantitative determination of miRNA.[66]

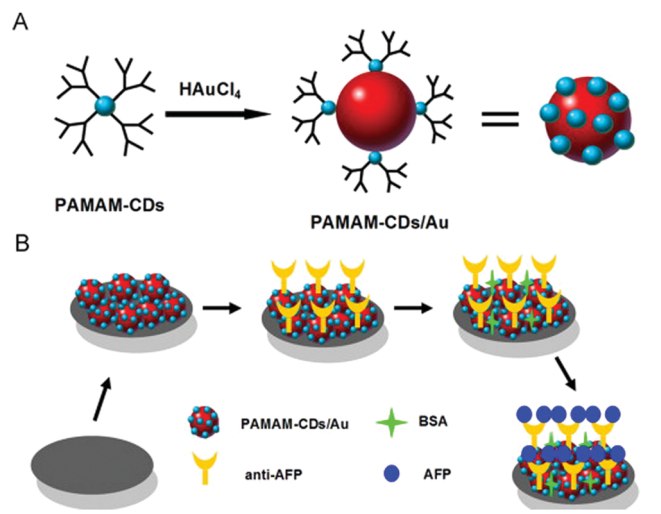

Fig. 4 The schematic diagram of the PAMAM–CDs/Au nanocrystal nanocomposites (A); and fabrication of the PAMAM–CDs/Au nanocrystal nanocomposite-based electrochemical immunosensor (B). Reprinted with permission from ref. 60. Copyright 2013 Elsevier.

4. Applications in electrochemiluminescence sensing

Since the first ECL property of semiconductor Si nanocrystals was discovered by Ding *et al.* by both annihilation and coreactant routes in 2002, a series of semiconductor nanomaterials have been demonstrated to possess excellent ECL properties, such as CdSe, CdTe and PbS quantum dots. Meanwhile, the related mechanisms of anodic and cathodic ECL of semiconductor nanomaterials have been proposed to explain these ECL phenomena. However, these semiconductor quantum dots usually have high toxicity and thus bring serious health and environmental concerns. As a consequence, exploiting environmental and biocompatible ECL nanoemitters has become an urgent goal to facilitate the development of ECL applications.

Carbon-based dots showed a few of distinguished features like low toxicity, good biocompatibility and "earth-abundant" nature, and were thereby regarded as promising ECL nanoemitters for environmental and biological analysis. Since the ECL performance (both annihilation and coreactant mechanisms) of carbon nanocrystals in the aqueous phase was discovered in 2009, carbon-based dots have become a popular ECL nanoemitter in the realm of ECL.[44,67,68] For the electron-transfer annihilation mechanism, active $CDs^{+\bullet}$ and $CDs^{-\bullet}$ were generated when the potential was scanned to positive and negative voltages, respectively. On the other hand, the coreactant ECL mechanism only relies on the scanning potential in the negative range with the "reduction–oxidation" coreactant,[69] for example, $S_2O_8^{2-}$. Recently, Long *et al.* proposed a novel ECL pathway called a "self-co-reactant" mechanism where the benzylic alcohol on the CDs surface changed into a strong reductant under the positive voltage and became the coreactant of CDs themselves.[70] The work displayed a unique perspective towards the fascinating structures and corresponding ECL properties of CDs.

However, the conventional CDs showed a relatively low ECL efficiency as a result of their intrinsic electronic band structure and the relaxation dynamics of charge carriers in excited states. Therefore, many researchers have attempted various approaches aiming at regulating the local electronic and chemical properties of CDs. One of the most promising methods is heteroatom doping such as nitrogen and sulfur.[71] For example, N doping can inject electrons into the conduction band and lift the Fermi level of CDs, or generate more surface traps and thus accelerate electron transfer between coreactants and CDs. As a result, the N-doped CDs usually display stronger ECL efficiency than that of pristine CDs. Wang *et al.* thoroughly studied the ECL properties of CDs with different nitrogen doping concentrations.[72] They found that doping nitrogen can tune the electronic structure of the CDs and lead to widened band gap and slower decay dynamics. Accordingly, the increasing probability of radiative recombination relative to nonradiative recombination promoted the ECL performance. In addition, Zhang *et al.* synthesized nitrogen and sulfur co-doped GDs (NS-GDs) *via* a one-pot pyrolysis approach using citric acid and L-cysteine as two precursors.[71] Owing to much more surface capturing centers of excitons for NS-GDs than that for pristine GDs, the NS-GDs can capture more holes from $SO_4^{\bullet -}$, leading to higher ECL efficiency. As a result, an ECL efficiency of 32% compared with the $Ru(bpy)_3^{2+}/K_2S_2O_8$ was achieved in NS-GDs/$K_2S_2O_8$ systems, which is also 5.8-fold enhanced in comparison with the same system of pristine GDs. Apart from the heteroatom doping strategy, the C-related dangling bonds and functional groups of CDs possessed considerable effect to regulate the ECL properties of CDs.[73] It is reported that the ECL activity of CDs can be significantly enhanced with the increase of the C-related dangling bonds, suggesting that the ECL emission of CDs partially arose from the C-related dangling bonds. This result is consistent with the well-known surface-state emission mechanism of semiconductor nanomaterials. Since the surface-state of CDs is very crucial for the ECL property, Qin *et al.* investigated ECL characteristic of various CDs with different oxygen containing functional groups on the surface.[74] The oxidized CDs, partially reduced CDs and fully reduced CDs all showed stable positively charged luminophores and unstable negatively charged luminophores. Nevertheless, the ECL behaviors were found to vary considerably with different oxidative degrees, where the ECL intensity of partially reduced CDs was weaker than that of CDs and oxidized CDs, and moreover the ECL intensity of fully reduced CDs was negligible. Such results demonstrated that the functional groups of CDs containing oxygen have an important impact on the ECL properties.

In recent years, carbon-based dots have demonstrated their potential in a range of ECL sensing applications.[75,76] According to the kinds of targeted analytes, the advances of carbon-based dot involved ECL sensing applications are introduced by the following categories, namely, metal ion sensing, small molecule sensing, protein sensing, DNA/RNA sensing and cell sensing.

4.1. Metal ion sensing

Metal ion analysis is a basic and important area in ECL sensing because some of the metal ions have an adverse impact on human health and environmental protection. So far many ECL sensors have been fabricated for the determination of a series of metal ions, including Cr^{6+}, S^{2-}, Fe^{2+}/Fe^{3+}, Cu^{2+}, Pb^{2+} and Cd^{2+}.[77–83] Zhang *et al.* observed a dual-peak ECL behavior of CDs in tetrabutyl ammonium bromide (TBAB) ethanol solution and applied it in iron ion detection.[79] They found that the electron injection into the conduction band of CDs led to the first ECL peak, and ion annihilation reactions produced another ECL peak.[79] According to their research, the first ECL peak showed higher sensitivity to the environment and thus was used for metallic ion detection with a detection limit of 7×10^{-7} M.[79] Interestingly, Wang *et al.* found that the anodic ECL signal of nitrogen and sulfur co-doped GDs can be greatly enhanced by cadmium sulfide QDs.[84] However, in the presence of Pb^{2+}, the amplified ECL emission can be quenched by Pb^{2+} in turn, and thus an ECL strategy for the sensitive determination of Pb^{2+} was established.

It is widely known that Hg^{2+} is one of the most hazardous heavy metallic pollutants and has serious influences on the environment and human health. Thus, the development of highly selective and sensitive Hg^{2+} sensors is of crucial importance. Given that Hg^{2+} possesses a special property of specific interaction with two DNA thymine bases (T) and forms a stable T–Hg^{2+}–T complex, Tang and coworkers fabricated an ECL sensor for the determination of Hg^{2+} by using a GD and gold nanoparticle hybrid as the signal probe, which displayed good performance for the detection of Hg^{2+} in actual tap water and human serum samples.[85] Apart from Hg^{2+}, lead ions (Pb^{2+}), even in a small amount, can cause serious organ damage to the brain and other body tissues.[86,87] Therefore, Xiong *et al.* developed N-doped CDs as the ECL emitter and Pd–Au hexoctahedra–DNA dendrimers, which not only significantly enhanced the ECL signal of the N-doped CDs on the electrode surface, but also captured Pb^{2+} and thus resulted in a switch-off of the signal.[88] The proposed biosensor possessed good sensitivity and accuracy for the determination of intracellular Pb^{2+}.

The molecular imprinting technique has attracted extensive attention in the analysis of small molecules and metal ions due to its high selectivity. Thus, Li *et al.* used CD composite nanomaterials as ECL emitters and molecularly imprinted polymers as recognition units for the determination of ultra-trace levels of cobalt ions (Co^{2+}), which affected growth and yield of plants as well as posed adverse influence on human health.[89] Hence, a dual recognition effect was employed for improving selectivity: the first recognition step relied on the interaction between cobalt ions and amino acid residues of bovine serum albumin (BSA); the second recognition step was attributed to the specific recognition sites for the BSA–Co^{2+} complex from the molecularly imprinted polymer. Because of the quenching effect of BSA–Co^{2+}, the ECL intensity of CD composite nanomaterials is strong after BSA–Co^{2+} was eluted from the molecularly imprinted polymer. In contrast, the ECL signal was quenched again when BSA–Co^{2+} was re-adsorbed onto the molecularly imprinted polymer, leading to a ''switch off'' of the ECL signal. Moreover, due to the dual recognition effect, the imprinted membrane had distinct structural features

compared with traditional molecularly imprinted polymers for the detection of single metal ion species, thereby considerably improving the selectivity of the sensor.

Conventional ECL strategies that rely on labels and single emission channels are vulnerable to external interference from the instrument and the environment. To detect the metal ions in an accurate and convenient way, Chen *et al.* developed a dual-potential ECL system with nitrogen-doped GDs as a single-luminophor,[90] which can react with $O_2^{\bullet -}$ and HO_2^- to generate anodic and cathodic ECL, respectively. In the presence of Co^{2+} ions, the anodic ECL intensity was amplified due to the catalytic activity of Co^{2+} ions, while the cathodic ECL intensity was quenched because Co^{2+} ions effectively eliminated the generation of excited nitrogen-doped GDs*. Therefore, an accurate and reliable sensor based on potential-resolved ECL without any labeling and additional coreactants was developed, and this sensor displayed high sensitivity and selectivity against other coexisting metal ions.

In addition to detecting single metal ions, some novel ECL sensors for multiple targeted metal ions were also developed based on various strategies. Considering that both Hg^{2+} and Pb^{2+} are severe environmental pollutants and have fatal risks to human health,[91] it is important to quantitatively monitor Hg^{2+} and Pb^{2+} simultaneously, which usually coexist in ambient air, water, soil, food and even biological systems. Since the first microfluidic paper-based sensing devices were fabricated for bioanalytical applications with a series of merits such as portability, small volumes of samples and rapid analysis,[92–94] paper-based sensors have been attractive for on-site diagnosis and point-of-care. Zhang *et al.* combined DNA nanoprobes and a 3D paper-based ECL device for the simultaneous detection of Hg^{2+} and Pb^{2+} using the stable T–Hg^{2+}–T complex and Pb^{2+}-stabilized G-quadruplex.[95] Also, a dual-label potential-resolved strategy was employed owing to the anodic ECL emission of $Ru(bpy)_3^{2+}$–gold nanoparticle aggregates and cathodic ECL emission of carbon nanocrystal coated silica nanoparticles. In the absence of Hg^{2+} and Pb^{2+}, the two DNA probes were in an open configuration and the two labels were far from the electrode surface, thus resulting in low ECL intensity. In contrast, Hg^{2+} and Pb^{2+} made the two DNA probes fold into the T–Hg^{2+}–T complex and Pb^{2+}-stabilized G-quadruplex, and thus narrowed the distance between ECL nano-emitters and the electrode surface. Accordingly, the ECL signal both in anodic and cathodic potential was enhanced significantly, which showed a positive relationship with the concentration of Hg^{2+} and Pb^{2+}, respectively. This simple and cost-effective sensor was successfully applied to detect two metal ions in lake water and human serum samples.

4.2. Small molecule sensing

Quantitative detection of small molecules is important in food safety, environmental issues, and disease diagnosis. Therefore, developing a series of sensors with high sensitivity and low cost is highly desirable to ensure public health and environmental protection. Because of the versatility and simplified instruments, ECL as a promising analytical approach has already attracted extensive attention in recent decades, especially for detection of small molecules.[96–109] Determination of glucose is of importance given that its concentration is essential for medical diagnostics and associated with many diseases. Therefore, Tian *et al.* fabricated a glucose sensor based on the quenching effect of H_2O_2 produced by the enzymatic oxidation of glucose.[110] After forming a thin film consisting of glucose oxidase, chitosan and GDs on the electrode surface, the ECL intensity of GDs decreased linearly with the increase of glucose concentration. In another work, Ran *et al.* reported N-doped CD and gold nanoparticle hybrids with excellent catalytic capability, rendering a highly active ECL property.[111] Then a glucose ECL sensor was designed based on the hybrid nanomaterials *via* the quenching effect of H_2O_2 from glucose and glucose oxidase. Because of the synergistic effect and ECL-RET between the gold nanocluster and GDs, the ECL intensity of hybrid materials displayed 2.6-fold increase compared with that of only gold nanoclusters or 40-fold compared with that of only GDs.[112] As a result, the gold nanocluster@GDs composite can act as an amplified ECL luminophore to fabricate a "signal-off" sensor for the detection of pentoxifylline.

As an important raw chemical, nitroaniline is of crucial importance for the synthesis of numerous chemical products, but it has strong toxicity and contaminates ground water and soil.[113] As a result, highly sensitive and selective sensors that rapidly and effectively detect nitroaniline are highly desirable regarding soil safety, environmental protection and food security.[114,115] Chen *et al.* fabricated a simple and straightforward ECL sensor for the detection of nitroaniline on the basis of the diazotization reaction *via* the catalysis of nitrogen-doped GDs.[116] Here, the nitrogen-doped GDs played two roles: as an ECL label and a catalyst in nitroaniline detection. The catalytic diazotization reaction of nitroaniline by nitrogen-doped GDs produced the reagent with azide groups, which resulted in the obvious ECL enhancement of nitrogen-doped GDs owing to radical inducement. Therefore, the elaborate nitroaniline sensor displayed a wide linear response and can be applied in real water samples with satisfactory results.

Conventional cathodic coreactants for GDs or CDs are highly limited to strongly oxidative $S_2O_8^{2-}$, which seriously restricts the application of carbon-based ECL sensors. Recently, a commonly used reducing reagent, sulfite (SO_3^{2-}), has been considered as a new type of coreactant besides $S_2O_8^{2-}$.[117] Given that the ECL signal of GDs/SO_3^{2-} could rapidly diminish in the presence of H_2O_2, simple ECL sensors have been proposed for the determination of H_2O_2 and other biological molecules like glucose.

As we know, the ferrocyanide–ferricyanide redox system can be regarded as the electron injector and hole injector in various possible reactions. Based on this principle, Niu *et al.* fabricated a solid-state ECL sensor through $Fe(CN)_6^{3-/4-}$ inducing ECL amplification of CDs and peroxydisulfate systems.[101] The $Fe(CN)_6^{3-/4-}$ system can effectively convert the CDs and $S_2O_8^{2-}$ into $CD^{\bullet -}$ and $SO_4^{\bullet -}$, resulting in a 10-fold ECL amplification. Because glutathione caused the interference of exciton recombination processes, the as-prepared ECL platform realized sensitive and selective detection of glutathione in the presence of other interfering substances.

In addition, bipolar electrodes as a signal reporting method can also be used to fabricate glucose sensors based on the

cathodic ECL emission of GDs.[118] The wireless nature of bipolar electrodes facilitated potential applications that are impossible or inconvenient to achieve using conventional wired electrodes. Wu *et al.* fabricated bifunctional S,N-codoped CDs, not only serving as ECL emitters but promoting the generation of reactive oxygen species to enhance ECL intensity as well.[119] Besides, the electrode was modified by tyrosinase, which can consume dissolved oxygen *via* a classic oxidation reaction and thus lead to the decrease of the ECL intensity of CDs. However, upon adding the target pesticide atrazine into the electrolyte, the ECL intensity significantly grew due to the inhibition effect of atrazine towards the catalytic performance of tyrosinase. As a result, the ECL intensity of S,N-codoped CDs increased with increasing concentration of atrazine, displaying two linear ranges from 0.0001 to 0.01 μg L^{-1} and 0.01 to 20 μg L^{-1} with a detection limit of 0.08 ng L^{-1}.

Although the ECL technique possesses high sensitivity and universality, its selectivity relies on the special recognition interaction or the pretreatment of extra separation. To improve the selectivity of ECL assays, Hu *et al.* combined magnetic solid phase microextraction with a ratiometric ECL detection of tetracycline using CDs and $Ru(bpy)_3^{2+}$.[120] Given that tetracycline possesses a strong affinity for zinc ions, they used nano-sorbent Fe_3O_4@SiO_2@ZnO to extract tetracycline in the complex sample. During the cathodic and anodic potential scanning, the $CD^{-\bullet}$ and $CD^{+\bullet}$ radicals as the coreactants can react with $Ru(bpy)_3^{+}$ and $Ru(bpy)_3^{3+}$ to generate excited state $Ru(bpy)_3^{2+*}$, leading to potential-resolved dual ECL emission. On the other hand, the tetracycline extracted by the sorbent can quench both cathodic and anodic ECL signals. More importantly, the ratio of the two signals is associated with the concentration of tetracycline with a 0.47 nM detection limit. Thus, this strategy showed excellent selectivity and accuracy owing to the prior separation and ratiometric ECL signals. Similarly, Chen *et al.* found that nicotinamide adenine dinucleotide (NADH) can amplify the anodic ECL intensity of N-doped GDs but diminish its cathodic ECL intensity.[121] Thus, a ratiometric ECL sensor was fabricated for the detection of NADH in biological sample matrixes.

Molecular imprinting polymers (MIP) have attracted extensive attention because of their potential application in molecular recognition. Moreover, combining MIP with other recognition techniques enables further improvement in selectivity and elimination of interference. Therefore, Li *et al.* used specific complexation between L-canavanine and trinitrobenzene as the first recognition, and MIP as the second recognition of the newly formed L-canavanine–trinitrobenzene complex.[122] The dual-recognition mechanism facilitated the selectivity of L-canavanine in this sensor where the L-canavanine–trinitrobenzene complex sufficiently quenched the ECL intensity of CDs on the electrode surface. Interestingly, Li *et al.* recently fabricated an aptamer-molecularly imprinted sensor *via* the aptamer–target interaction for the determination of lincomycin.[123] The CD-labelled DNA aptamers, lincomycin, and *o*-aminophenol underwent electropolymerization and formed an imprinted polymer on the electrode modified with gold nanoparticles and graphene oxide (Au–GO). After the elution of lincomycin, the CDs showed enhanced ECL signals due to the ECL-RET between Au–GO and CDs. In contrast, when lincomycin was bound to the DNA aptamer in the imprinted polymer, it blocked the energy transfer and resulted in a decrease of ECL intensity. Therefore, this strategy was utilized to monitor lincomycin residuals in real meat samples with satisfactory results. Because molybdenum disulfide (MoS_2) has a specific 2D layered feature, electronic properties and unique physical and chemical properties, the CDs/MoS_2 hybridization exhibited 13-fold enhancement of ECL intensity in comparison to CDs.[124] The superior ECL emitters combined with molecularly imprinted polymers showed high sensitivity and stability for the determination of 2-methyl-4-chlorophenoxyacetic acid, indicating the promising applications for the detection of other drugs and pesticides.

As a wide strategy used in luminescence techniques, RET opens up a new avenue to fabricate ECL sensors with more flexibility, such as distance-dependent ECL assay and spectra-based ratiometric ECL.[125] Due to the tunable luminescence properties of GDs, Tian *et al.* developed an ECL-RET system with N-doped GDs as the acceptor and luminol as the donor.[126] Notably, the luminol and N-doped GD hybrids can generate anodic ECL signals without coreactants. Given that reactive oxygen species can facilitate the oxidation of luminol and thus enhance the ECL intensity, an ECL approach for sensitively detecting H_2O_2 was performed and applied to the detection of H_2O_2 in real water samples. Aptamer-based biosensors have attracted much attention due to the versatile target and low cost of aptamers,[127] so Li *et al.* fabricated an aptamer sensor for carbofuran detection on the basis of the ECL energy transfer between fullerene C60-loaded Au nanoparticles and CDs.[128] After specifically binding with the DNA aptamer, carbofuran blocked energy transfer and decreased the ECL intensity because the change of the tertiary structure of the DNA aptamer by binding the target caused the CDs labeled on the aptamer to move far away from the electrode surface. The decreasing ECL signal showed a linear correlation with the carbofuran concentration, thereby establishing a new method for quantitative analysis.

The combination of two or more types of signals for quantitatively detecting some crucial biomarkers enabled preliminary screenings and accurate determination. Wang *et al.* developed a dual channel method for ochratoxin A (OTA) detection *via* the combination approach with enriched surface-state ECL and homogeneous fluorescence detection.[129] The event that the aptamer anchoring on the magnetic beads specifically interacted with OTA led to the dissociation between preloaded nitrogen-doped GDs@SiO_2 nanoparticles and magnetic beads. After the magnetic separation, therefore, the fluorescence signal of residual nitrogen-doped GDs in the homogeneous bulk solution went up while the ECL signal from the magnetic electrode surface decreased. On one hand, ECL measurements provided higher sensitivity and a cheaper instrument for more accurate results. On the other hand, fluorescence assay showed a wide dynamic range and better stability thanks to the homogeneous detection. Integrating the merits of two different analytical strategies, this proposed aptasensor opened up a new avenue in designing other sensors with dual channels.

In addition to a versatile ECL nano-emitter, GDs with abundant functional groups like alcohol units[130] and tertiary amino groups[131] have been successfully used as coreactants of $Ru(bpy)_3^{2+}$ and displayed the capacity as effective alternatives to tripropylamine (TPrA).[132–135] Considering the high toxicity and volatility of TPrA, GDs with good solubility and high chemical stability are excellent candidates to fabricate sensors. As a result, a series of ECL sensors based on this strategy have been developed to detect small molecules.[136] For instance, as a typical class of persistent organic pollutants in our environment, chlorinated phenols have obvious adverse effects on human health.[137] Taking advantage of the quenching effect of chlorinated phenols toward the ECL reaction between GDs and $Ru(bpy)_3^{2+}$, Qi *et al.* fabricated a chlorinated phenol sensor with good performance even in lake and river water.[130] Besides, Li *et al.* made a bisphenol A sensor based on a similar mechanism, where bisphenol A inhibited the ECL intensity with $Ru(bpy)_3^{2+}$ as the luminophore and N-doped CDs as the coreactant.[133]

To further enhance the effect of CDs as the coreactant, Li *et al.* synthesized poly(ethylenimine) (PEI) capped N-doped CDs, which exhibited a better enhancement effect than naked N-doped CDs.[138] Consequently, the double enhancement contribution of PEI and N-doped CDs enabled the amplification of ECL signals and better detection sensitivity for analyzing diphenol compounds. Except for enhancing the ECL intensity of $Ru(bpy)_3^{2+}$ molecules, N-doped GDs can also act as the coreactant to enhance the $Ru(bpy)_3^{2+}$-doped silica nanoparticles (RuDSNs).[135] Accordingly, a self-enhanced ECL nano-emitter was constructed by electrostatic conjugation between RuDSNs and N-doped GDs and then a modification at the electrode surface. After binding with the aptamer of zearalenone, the self-enhanced ECL aptasensor showed a gradually decreasing ECL intensity with increasing zearalenone concentration, which was attributed to the rise of electrochemical impedance. Recently, Nie *et al.* synthesized nitrogen-rich quantum dots (N-dots) with much higher nitrogen content than that in N-doped CDs, thereby significantly increasing the reactive sites for the ECL reaction on the surface of N-dots.[139] Thus novel N-dots were used to design the enzyme sensor that accurately quantifies galactose *via* H_2O_2 as the coreactant modifier.

4.3. Protein sensing

Commercial ECL instruments have widely been used to detect crucial clinical disease biomarkers, most of which depend on the high affinity of the antigen–antibody interaction for high selectivity. In addition, the ECL technique provides a series of advantages like low background, simplified setup and high sensitivity, enabling the trace detection of many low abundant biomarkers in bio-samples,[140] such as carbohydrate antigen 199,[141] carcinoembryonic antigen,[142] cancer antigen 125,[143] squamous cell carcinoma antigen[144] and prostate protein antigen.[145] For example, thrombin as a widely used model protein plays a crucial role in blood agglomeration. Du *et al.* used nitrogen-doped GD doped silica nanoparticles as the ECL labels and the thrombin aptamer as the recognition units for fabrication of thrombin aptasensors.[146] The specific binding between thrombin and thrombin aptamer labeled by nitrogen-doped GD doped silica nanoparticles resulted in the dissociation of ECL emitters from the electrode surface, along with a significant decrease in the ECL intensity. As a consequence, the ECL aptasensor exhibited a low detection limit and high selectivity in serum samples, thereby demonstrating the promising application for detecting thrombin in other complex samples. Besides, because the interaction between aptamers and specific proteins would lead to the increase of electrochemical impedance, some label-free ECL aptasensor was developed for the detection of thrombin and lysozyme by monitoring the ECL decrease of N-doped GDs on the electrode surface after the binding event.[147,148] Based on the quenching effect of CdTe nanoparticles modified with Fe_3O_4 magnetic nanoparticles toward TiO_2 nanotube arrays filled with GDs, Tian *et al.* fabricated a "turn-off" ECL sensor for the determination of prostate protein antigen by a classic sandwich immunoassay.[149] To reduce the anodic ECL potential, a new nano-hybrid of hydrazide-modified GDs and gold nanoparticles was synthesized and showed excellent anodic ECL performance at a low potential below 0.8 V with H_2O_2 as the coreactant.[150] The superior composites on the electrode surface were modified with carcinoembryonic antibody to capture the corresponding antigen. With the increment of electron-transfer resistance after the sandwich immunoreaction, the ECL intensity gradually decreased, thereby realizing the quantitative detection of carcinoembryonic antigen.

Similarly, Zhu *et al.* reported a RET strategy based on N-doped GDs/$Ni(OH)_2$ with a three-dimensional hierarchical and stacked lamellar structure as the ECL donor and Fe_3O_4@MnO_2 composites with a wide absorption range as the ECL acceptor.[151] After the sandwich immunoassay *via* a specific antigen–antibody interaction, the ECL intensity of N-doped GDs on the electrode surface was quenched and the variable can be used to realize reliable detection of prostate protein antigen in real serum samples with good recoveries.

Protein kinases play a critical regulatory role in many fundamental biological processes and abnormal expression has been implicated in a large number of diseases such as cancers, HIV and Alzheimer's disease. The evaluation of kinase activities and investigation of their potential inhibitors are valuable for the discovery of kinase-targeted drugs. When peptides on the surface of GD modified electrode were phosphorylated in the presence of casein kinase 2 (CK2) and adenosine 5′-triphosphate (ATP), the anti-phosphoserine antibody conjugated graphene nanocomposite was captured onto the phosphorylated peptide/GD electrode surface, leading to ECL quenching of GDs. The ECL quenching was positively correlated with CK2 activity.[152]

Because the ECL intensity of CDs is closely associated with the homogeneous reactions between electrochemically reduced intermediates of CDs and oxidant radical $SO_4^{\bullet -}$, any species promoting the generation of oxidant radical $SO_4^{\bullet -}$ can enhance the ECL signal. Based on this strategy, Dong *et al.* fabricated an ECL sensor for the determination of cytochrome *c* by using CDs as the cathodic ECL nano-emitters.[153] Spectral and

electrochemical studies showed that cytochrome *c* had the ability of reducing potassium persulfate to oxidant radical $SO_4^{\bullet -}$. This strategy enabled one to detect cytochrome *c* with satisfactory sensitivity and selectivity.

Although the cathodic ECL emission of GDs has been widely investigated, there are relatively few studies devoted to the anodic ECL of GDs due to its weak and unstable signals. Cai *et al.* developed a strategy of chemical and electrochemical co-mediation for a significant ECL enhancement of GDs at both the anode and cathode.[154] In other words, dual potential ECL was achieved by one GD nano-emitter and two different coreactants of $K_2S_2O_8$ and Na_2SO_3. Furthermore, an ECL immunosensor on the basis of the novel dual-potential ECL mechanism was fabricated for the determination of HIgG with satisfactory sensitivity because the captured HIgG led to an increase of the electrochemical impedance of the GDs modified electrode.

To further improve the sensitivity of ECL immunosensors, a double-quenching approach was proposed for the detection of protein kinase A (PKA).[155] In this strategy, a GD coated ITO electrode possessed a strong and steady ECL intensity with H_2O_2 as the coreactant. However, in the presence of PKA, the peptide anchored onto the electrode surface was phosphorylated, leading to a combination of gold nanoparticles and G-quadruplex–hemin DNAzyme. Because of the catalytic decomposition of H_2O_2 by DNAzyme and the energy transfer between GDs and gold nanoparticles, the ECL intensity of GDs was considerably suppressed. The double-quenching ''turn off'' strategy realized excellent analytical performance in serum samples and cell lysates.

In addition to the ''turn off'' strategies for fabricating ECL sensors, GDs can be used as a label to conjugate with the secondary antibody and thus enhance ECL intensity after the sandwich immune reactions.[156] Based on the signal-on strategy, Nie *et al.* designed superior poly(5-formylindole)/reduced graphene oxide nanocomposites to facilitate ion transport and increase surface areas, and gold nanoparticle decorated GDs to improve electron transfer capability with a stable ECL intensity.[157] Results demonstrated that the strategy can be used to detect carcinoembryonic antigen with a broad linear range and a low detection limit, thereby possessing good performance in serum samples. Also, Qin *et al.* used a graphene oxide–polyethylenimine–CDs–Au nanohybrid as the signal probe to measure carbohydrate antigen 15-3 (a breast cancer biomarker) in human serum based on the sandwich immunoassay with the synergistic action of the active electrode substrate and the signal probe.[158] Furthermore, based on immunoassay or aptamer-based ECL strategies, researchers developed a variety of other ECL sensors for the detection of proteins like concanavaline A, thrombin, and carcinoembryonic antigen.[159,160]

In addition, another kind of ECL nanocomposite assembled by dual luminophores was developed while most reported ECL sensors merely depend on mono-luminophore.[161] The proposed synergistic effect significantly enhanced the ECL intensity so that the fabricated immunosensor exhibited excellent sensitivity and a broad linear range for the determination of carcinoembryonic antigen. On the other hand, dual luminophores provided an opportunity to design the potential-resolved ECL ratiometric method by using gold nanoparticles as signal transduction units for regulating the cathodic ECL signal of GDs and the anodic ECL signal of luminol.[162] The GDs were first modified on the electrode surface and then conjugated with peptides. In the presence of adenosine 5′-[γ-thio]triphosphate (ATP-s) and protein kinase, the peptides were phosphorylated to form thiophosphorylated peptides, and then specifically captured gold nanoparticles, which quenched the ECL of GDs owing to RET. In contrast, the ECL intensity from luminol in the electrolyte can be enhanced by the same gold nanoparticles with good electrocatalytic activity. As a result, the ratio of the ECL signals from CDs and luminol showed a correlation with the activity of protein kinase.

Recently, various paper-based sensors and devices have been developed in the field of fluorescence, electrochemistry, and chemiluminescence due to their low cost, portability and flexibility.[163–165] Zhang *et al.* fabricated an ultrasensitive ECL paper sensor using nitrogen-doped GDs for the detection of α-fetoprotein.[166] When employing multi-walled carbon nanotubes as the carriers of nitrogen-doped GDs to amplify ECL signal and a gold nanoflower modified paper working electrode with a porous morphology to increase the surface area and conductivity, the paper-based immunodevice showed high sensitivity and reproducibility for quantitative detection of α-fetoprotein *via* the classic antigen–antibody interaction. To further improve the selectivity for the determination of α-fetoprotein, a boronate affinity molecular imprinting technique was used based on SiO_2/CDs/gold nanoparticle composites as the ECL labels.[167] The proposed ECL sensor showed excellent performance, especially in terms of selectivity in serum samples, indicating its great potential for application in clinical diagnostics. Rolling circle amplification (RCA) has been often used as an isothermal amplification procedure to produce a linear concatenated DNA molecule containing up to 1000 complementary copies of the circular DNA. Thus, a powerful immune-RCA assay strategy was conducted for the detection of human IgG by combining the CDs conjugated to DNA probes and the amplification ability of the RCA.[168] The proposed approach displayed significantly amplifying ECL intensity as well as high stability and accuracy.

It was commonly agreed that the determination of multiple disease markers in parallel can significantly improve the accuracy and effectiveness of disease diagnosis.[169–171] Accordingly, Zhou *et al.* developed a potential-resolved ECL sensor (Fig. 5) for simultaneous detection of triple latent tuberculosis infection markers, namely, interferon-gamma (IFN-γ), tumor necrosis factor-alpha (TNF-α), and interleukin-2 (IL-2).[172] In this work, gold nanoparticles modified with luminol, CDs and CdS QDs respectively can be used as three ECL nanoprobes to detect the corresponding three targets. A patterned ITO electrode provided spatially resolved regions for these three nanoprobes. Thanks to the potential-resolved ECL signals of these three nanoprobes (luminol at +0.6 V, CdS at −1.2 V and CDs at −1.8 V), the binding reaction of antibody-functionalized ECL nanoprobes can indicate the concentration of IFN-γ, TNF-α and IL-2 in human serum, thereby facilitating more accurate and reliable clinical diagnosis for triple latent tuberculosis infection. Furthermore, a

microfluidic paper-based ECL immune-device showed the capability to diagnose of four cancer biomarkers (α-fetoprotein, carcinoma antigen 153, carcino embryonic antigen and carcinoma antigen 199) simultaneously based on a two-electrode system.[173] Based on a potential-resolution strategy with CDs and $Ru(bpy)_3^{2+}$ as the ECL labels for high throughput ECL immunoassay, the detection of four cancer biomarkers was achieved even in human serum samples. The novel strategy provided a promising technique for multiplex immunoassay and point-of-care diagnosis.

4.4. DNA/RNA sensing

Nucleic acids such as p53 gene,[174,175] mitochondrial DNA,[176] and human papillomavirus type 16 DNA[177] are closely associated with many diseases and clinical diagnostics.[178,179] However, these crucial nucleic acids often have low abundance in real biological samples.[180] Hence a number of DNA amplification techniques have been designed to improve the detection sensitivity and achieve trace level analysis. Different DNA cascade reactions, such as the hybridization chain reaction,[181] catalytic hairpin assembly[182] and primer exchange reaction,[183] have provided a large number of signal amplification techniques for improving the sensitivity. Also, some classic approaches like strand displacement amplification,[184] polymerase chain reaction,[185] and endonuclease-aided amplification[186] have drawn great attention of researchers, both in the electrochemical and optical fields.[187] For example, in order to combine the DNA amplification techniques with ECL techniques of GDs, Jie *et al.* developed a DNA sensor using GDs as the ECL nano-emitters and an endonuclease-assisted cyclic amplification strategy to improve the sensitivity.[188] The proposed ECL sensor outperformed other optical-based methods and can be potentially applied to real samples owing to good selectivity and sensitivity. In addition, site-specific cleavage of *Bam*HI endonuclease can be used to fabricate ECL signal amplification systems, so a novel signal-off DNA biosensor was developed to detect hepatitis C virus-1b genotype complementary on the basis of *Bam*HI endonuclease.[189] Using GD as a label and an ECL nano-emitter, *Bam*HI endonuclease recognized the duplex symmetrical sequence and catalyzed dsDNA cleavage, resulting in GDs moving away from the electrode surface and a decrease of the ECL intensity. Wang *et al.* designed a "turn off" DNA biosensor based on the enhanced ECL performance of hydrazide modified GDs and the catalytic activity of hemin/G-quadruplex DNAzyme.[190] Given that hemin/G-quadruplex DNAzyme can effectively catalyze the decomposition of H_2O_2, the target p53 DNA can thus be determined by manipulating the formation of hemin/G-quadruplex DNAzyme, and then led to the ECL decrease because the H_2O_2 acted as the coreactant of GDs on the electrode surface. Using this proposed biosensor, p53 gene can be quantified with desirable stability and high selectivity in discrimination of single-base mismatch.

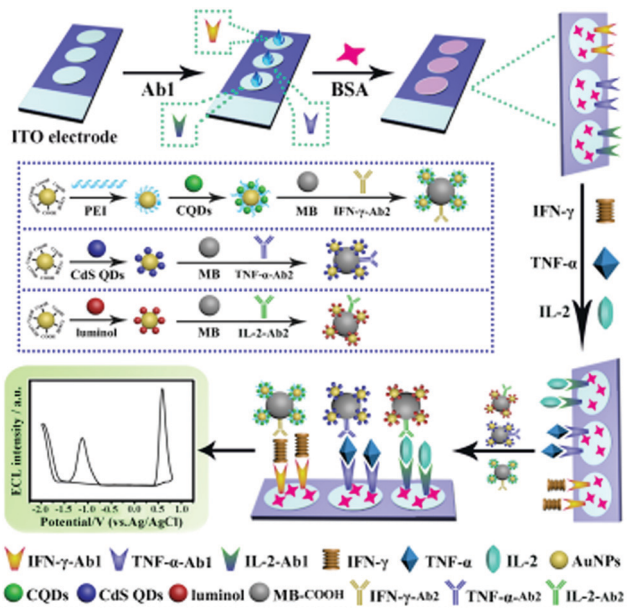

Fig. 5 Preparation and schematic illustration of the multiplexed ECL immunosensor for simultaneous detection of IFN-γ, TNF-α and IL-2. Reprinted with permission from ref. 172. Copyright 2017 American Chemical Society.

MicroRNAs (miRNAs) are a class of small noncoding RNA molecules and have important effects in gene expression in many crucial physiological processes. Increasing evidence indicates the close relationship between aberrant repression of miRNAs and many fatal diseases. However, the low abundance of miRNA in biological samples raised a great challenge for the sensitive techniques. Therefore, many researchers combined the ECL technique with various DNA amplification techniques to realize the quantitative analysis of miRNA.[191] Zhang *et al.* synthesized boron doped graphene quantum dots (BGDs) for the detection of miRNA-20a by the spatial transformation of hairpin DNA after hybridization with a target miRNA-20a.[192] Furthermore, Liu *et al.* developed a miRNAs biosensor based on the target-triggered cycling amplification with a nicking enzyme and highly efficient ECL emission of nitrogen-doped CDs.[193] The hairpin probe binding with assistant DNA and target miRNA can form a Y-shaped structure which nicking enzymes cleaved to release miRNA and further triggered the next recycling process. The residual DNA labelled nitrogen-doped CDs subsequently hybridized with the hairpin probes immobilized on the electrode surface, resulting in the enhancement of ECL intensity. Due to the efficient signal amplification of the target-induced cycling reaction, the CD-based miRNA biosensor displayed a wide detection range and low detection limit. Similarly, an ECL method based on an efficient coreactant accelerator mechanism for sensitive determination of miRNA-21 was developed through a T7 exonuclease-assisted target recycling and hemin/G-wire for enhancing the ECL efficiency of CDs.[194] After cleavage by T7 exonuclease, the G-quadruplexes/hemin on the electrode catalyzed the reaction of peroxothiosulfate and facilitated the ECL efficiency of CDs on the electrode surface. This work opened up a promising strategy by combining nucleic acid amplification and a co-reaction accelerator in ECL systems.

It has been widely demonstrated that a highly up-regulated long non-coding RNA (IncRNA) can be used as a non-invasive biomarker for early diagnosis of hepatocellular carcinoma. However, searching for a cheap and effective strategy for detecting this IncRNA in the early stage of liver cancer remains challenging.[195] So Li *et al.* developed a highly sensitive ECL

sensor using Au@Ag core–shell nanoparticles/GDs as the ECL indicator to detect IncRNA.[196] In comparison to only Au or Ag nanoparticles, the hybrid nanocomposite displayed larger surface area and faster electron transfer owing to the synergistic effect between the two noble metals. Consequently, the ECL intensity of GDs was greatly amplified, and the proposed ECL sensor based on the DNA sandwich hybridization reactions showed a low detection limit and wide linear range.

4.5. Cell sensing

Sensitive and accurate identification and detection of cancer cells is of importance to early diagnosis and timely treatment for potential patients. Because the ECL technique possessed a variety of merits of low background, simplicity and high sensitivity, an aptamer-based ECL sensor for the detection of MCF-7 breast cancer cells was developed with CD coated mesoporous silica nanoparticles as the ECL tracers because of its high biocompatibility.[197] A three-dimensional graphene and gold nanoparticle hybrid nanostructure as the electrode substrate was modified with concanavalin for the capture of MCF-7 cells. Subsequently, the ECL tracer with mucin1 aptamer specifically interacted with mucin1 on the cell membrane and indicated the number of cells according to the increase of ECL intensity. In another work, Zhang *et al.* used the sandwich reaction for the determination of K562 leukemia cells by using CD coated ZnO nanospheres as the ECL probe and an aptamer as the recognition unit.[198] Due to the intrinsic insulation of cancer cells, the ECL emitters on the electrode surface probably showed decreasing ECL intensity after selectively capturing the cells *via* the specific recognition units. Wu *et al.* fabricated CDs and Ag nanoparticle hybrids as the electrode substrate that showed a bright ECL signal in the absence of cells.[199] After the folic acid on the hybrids recognized folic acid receptors on the membrane of human cervical cancer cells or human breast cancer cells, the ECL intensity of CDs and Ag nanoparticle hybrids decreased significantly. The ECL cytosensor showed a wide linear range and a low detection limit for cancer cells.

The identification and measurement of tumor biomarkers hold significant promise for the early detection of cancer and therapy monitoring. The expression patterns of surface antigens on cells are associated with various diseases. Liu *et al.* performed a low potential triggered microfluidic paper-based analytical device for the determination of carbohydrate antigen 153 on MCF-7 cells. Based on GD loaded surface villous Au nanocages as the ECL signal probe, the sandwich-type sensor was fabricated to *in situ* and accurately analyze the antigen on the cell surface.[200] Because most of the CDs only possessed relatively low ECL intensity, Qiu *et al.* developed a solid-state zinc-coadsorbed CD nanocomposite (ZnCDs) as an ECL probe to detect breast cancer cells and evaluate the CD44 expression level.[201] After the attachment of ZnCDs to gold nanoparticles and then the loading of magnetic beads to amplify the ECL intensity, the probe displayed a significant 120-fold increase of the ECL signal. Accordingly, hyaluronic acid-functionalized solid-state probes can be used as a super-label to specifically recognize CD44 on the MDA-MB-231 and MCF-7 cells, revealing a good analytical performance to study the individual cellular function and cellular heterogeneity. In addition to developing advanced ECL nanoemitters for cell analysis, a suitable space between ECL probes and electrode surface is equally important for effective nanoprobe labelling. As a result, a single-cell sensor with a spatial architecture was studied for achieving optimal single-cell ECL analytical performance *via* mercapto acids with different carbon chain lengths as the bridge (Fig. 6).[202] Eventually, 11-mercaptoundecanoic acid was selected to offer optimal interspace on the electrode surface and facilitated the ECL intensity of lead-coadsorbed CDs, which specifically recognized the CD44 receptor on the cell surface as the ECL reporter. Thus, the novel strategy provided a single-cell analysis platform to acquire high-precision analytical results and evaluate the cellular heterogeneity and biological function.

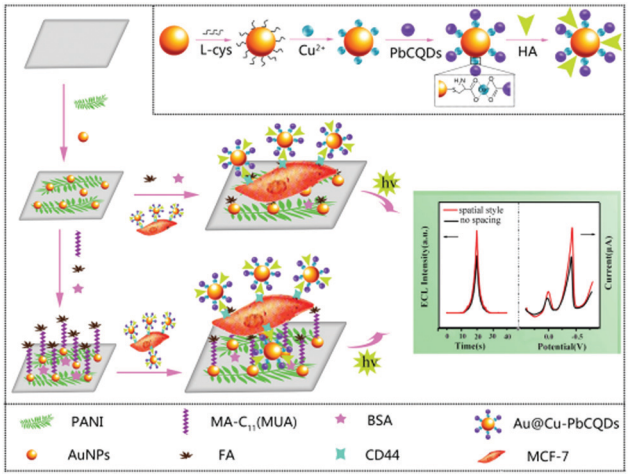

Fig. 6 Preparation process of the bifunctional Au@Cu–PbCQD nanoprobes and the fabrication of the MUA-spaced single-cell sensor. Reprinted with permission from ref. 202. Copyright 2018 Royal Society of Chemistry.

Apart from the detection of cancer cells, paper-based analytical devices also showed the capacity of *in situ* screening of anticancer drugs by the combination between ECL and fluorescence techniques. Wu *et al.* fabricated PtNi alloys for high loading of CDs as the ECL label, which can further recognize MCF-7 cells through 3D in-electrode cell culture.[203] The paper-based ECL cyto-device exhibited excellent performance as a cyto-sensing platform. Moreover, paclitaxel, fluorouracil and cisplatin were selected as model drugs for the induction of apoptosis of MCF-7 cells. The fluorescence images showed that the fluorescence intensity varied considerably with three drugs using FITC-annexin-V as the fluorescence bioprobe, suggesting the heterogeneous anticancer effect of different drugs.

Adhesion of platelets to endothelial cells played a crucial role in cardiovascular diseases, and thus the studies about platelet adhesion to endothelial cells with oxidative damage are beneficial to the understanding of cardiovascular diseases. Long *et al.* fabricated an ECL-based cell sensor using the adhesion molecule on the damaged human umbilical vein endothelial cell as the biomarker site and CDs as the nanoprobe.[204] When the platelets were activated by collagen stimuli, the adhesive potential of platelets to the damaged endothelial cells became firm, leading to the decrease of the ECL intensity of CDs on the cell surface, and thus quantitatively detecting the

figure for platelet adhesion to a single cell. Moreover, to expand the applications in drug analysis, the ECL platform was further applied to the studies of platelet adhesion to single cells under various drug stimuli, including the inhibitors of aspirin, heparin and quercetin. These results demonstrated the versatility of the single-cell analysis platform for studying single intercellular adhesion.

In order to provide multifunctions including specific reagent storage, multiple sample immobilization, residual automatic washing, and signal collection, Yang *et al.* designed and constructed a sudoku-like lab-on-paper platform for multiplexed competitive ECL cyto-assay.[205] To prove this concept, MCF-7, K562, HeLa, and CCRF-CEM cells were used as proof-of-concept cell lines to investigate the performance of the device. Upon converting the cell concentration into the final loading amount of the light-switch silver nanoparticle/DNA/GDs hybrid, simultaneous and ultrasensitive detection of four types of cancer cells was achieved on the four different regions of the sudoku-like origami-based ECL cyto-device.

Escherichia coli (*E. coli*) is a common and fatal pathogenic bacterium causing a series of diseases including hemolytic uremic syndrome, hemorrhagic colitis and so on. There is thereby an urgent need, but it has so far been a significant challenge, to detect *E. coli* in a convenient way. Considering that the ECL measurement merely depends on the voltage to induce luminescence rather than peripheral circuits to measure current, Li *et al.* developed an intriguing smartphone-based ECL system for the detection of *E. coli* using a universal serial bus interface to provide voltage, and a camera to capture luminescence.[206] Furthermore, using GDs to amplify and stabilize the ECL signals, they developed a smartphone-based image analysis application for image processing. Due to the insulation of *E. coli*, the ECL images on the smartphone diminished gradually after *E. coli* was captured by the antibody and thus led to the increase of impedance. Thanks to the integration of portable smartphones, this technique showed a promising application in point-of-care testing.

Escherichia coli O157:H7 can cause serious illnesses and conventional detection methods for its determination are substantially time-consuming and require expensive equipment.[207,208] Therefore, a facilely prepared ECL biosensor with a surface imprinted polymer as the recognition units and N-doped GDs as the ECL emitters was developed based on a sandwiched configuration.[209] The dopamine and target bacteria were electropolymerized directly on the electrode to form imprinted polymer films, followed by the removal of the bacteria template. After selectively recognizing with *Escherichia coli* O157:H7, its polyclonal antibody labeled with N doped-GDs interacted with *Escherichia coli* O157:H7 and thus generated intensive ECL irradiation. Consequently, the proposed bacteria sensor displayed high selectivity and a wide linear range.

5. Summary and prospects

As mentioned above, the marriage between carbon-based dots and the ECL technique opens a promising avenue in not only gaining insight into the fascinating electrochemical and optical properties of carbon-based dots but the fabrication of high performance ECL sensors as well. As we know, the development of novel nanomaterials constantly provides infinite possibility for the design of superior ECL sensors. Carbon-based quantum dots with chemical inertness, good solubility and high biocompatibility have attracted extensive attention in the realm of ECL over the last decade. Compared with the traditional $Ru(bpy)_3^{2+}$ system, carbon-based quantum dots show more stable ECL emissions during the continuous potential scans. Among the quantum dots, carbon-based quantum dots possess the advantages of low toxicity and high biocompatibility relative to classical chalcogenide quantum dots. More importantly, the tailored surface functional groups enable various modification of other advanced nanomaterials and biomolecules like DNA, proteins and other active groups. This review has summarized ECL sensors with carbon-based quantum dots for the detection of metal ions, small molecules, proteins, nucleic acids and cells. Nevertheless, the potential applications based on the ECL properties of carbon-based quantum dots are far more than the content of this review. We believe there is still plenty of room for the development of both novel carbon-based quantum dots and sensing methodologies in the near future.

In spite of these burgeoning achievements of ECL sensors based on carbon-based quantum dots, it is worthwhile mentioning that there is an urgent need, but it is still a significant challenge, to rationally design and delicately tailor carbon-based quantum dots with high-efficient ECL emission. Both heteroatom-doping strategy and energy transfer process have established themselves as promising approaches to improve the ECL efficiency of carbon-based quantum dots. Additionally, an elaborate electrode configuration also plays an irreplaceable role in advanced ECL sensors, such as bipolar electrodes and paper-based electrodes. We expect that ultramicroelectrode arrays and self-powered sensors could be the next hotspot for ECL sensing electrodes. Considering that ECL detectors so far have often been limited to photomultiplier tubes, other advanced ECL detectors like spectrometers[210] and CCD cameras[211,212] show more fascinating merits such as spatiotemporal resolution and high throughput. Therefore, advanced ECL instruments could promote the development of carbon-based quantum dots for ECL sensing in the future.

Conflicts of interest

The authors declare no competing financial interest.

Acknowledgements

This research is supported by the National Natural Science Foundation of China (Grants No. 21904063), the Natural Science Foundation of Jiangsu Province (Grants No. BK20190279), and the International Cooperation Foundation from the Ministry of Science and Technology (2016YFE0130100).

References

1 L. Ma, K. E. Hendrickson, S. Wei and L. A. Archer, *Nano Today*, 2015, **10**, 315–338.
2 F. Perreault, A. F. De Faria and M. Elimelech, *Chem. Soc. Rev.*, 2015, **44**, 5861–5896.
3 X. Yang, M. Yang, B. Pang, M. Vara and Y. Xia, *Chem. Rev.*, 2015, **115**, 10410–10488.
4 Y. Chen, S. Zhou, L. Li and J. J. Zhu, *Nano Today*, 2017, **12**, 98–115.
5 Y. Cao, Z. Zhang, L. Li, J. R. Zhang and J. J. Zhu, *Anal. Chem.*, 2019, **91**, 8607–8614.
6 R. Wang, K. Q. Lu, Z. R. Tang and Y. J. Xu, *J. Mater. Chem. A*, 2017, **5**, 3717–3734.
7 X. Li, M. Rui, J. Song, Z. Shen and H. Zeng, *Adv. Funct. Mater.*, 2015, **25**, 4929–4947.
8 Z. Fan, S. Li, F. Yuan and L. Fan, *RSC Adv.*, 2015, **5**, 19773–19789.
9 C. D. García, A. G. Crevillén and A. Escarpa, *Carbon-based Nanomaterials in Analytical Chemistry*, Royal Society of Chemistry, 2018.
10 A. J. Bard, *Electrogenerated chemiluminescence*, CRC Press, 2004.
11 M. M. Richter, *Chem. Rev.*, 2004, **104**, 3003–3036.
12 Z. Liu, W. Qi and G. Xu, *Chem. Soc. Rev.*, 2015, **44**, 3117–3142.
13 L. Li, Y. Chen and J.-J. Zhu, *Anal. Chem.*, 2017, **89**, 358–371.
14 H. Sun, L. Wu, W. Wei and X. Qu, *Mater. Today*, 2013, **16**, 433–442.
15 Y. Xu, J. Liu, C. Gao and E. Wang, *Electrochem. Commun.*, 2014, **48**, 151–154.
16 L. Li, G. Wu, G. Yang, J. Peng, J. Zhao and J. J. Zhu, *Nanoscale*, 2013, **5**, 4015–4039.
17 W. Kwon, Y. H. Kim, C. L. Lee, M. Lee, H. C. Choi, T. W. Lee and S. W. Rhee, *Nano Lett.*, 2014, **14**, 1306–1311.
18 Y. Feng, C. Dai, J. Lei, H. Ju and Y. Cheng, *Anal. Chem.*, 2015, **88**, 845–850.
19 D. Sun, R. Ban, P. H. Zhang, G. H. Wu, J. R. Zhang and J. J. Zhu, *Carbon*, 2013, **64**, 424–434.
20 L. Wang, W. Li, B. Wu, Z. Li, S. Wang, Y. Liu, D. Pan and M. Wu, *Chem. Eng. J.*, 2016, **300**, 75–82.
21 S. N. Baker and G. A. Baker, *Angew. Chem., Int. Ed.*, 2010, **49**, 6726–6744.
22 J. Zhang and S. H. Yu, *Mater. Today*, 2016, **19**, 382–393.
23 X. Sun and Y. Lei, *TrAC, Trends Anal. Chem.*, 2017, **89**, 163–180.
24 R. Westervelt, *Science*, 2008, **320**, 324–325.
25 X. T. Zheng, A. Ananthanarayanan, K. Q. Luo and P. Chen, *Small*, 2015, **11**, 1620–1636.
26 Z. Zhou, L. Xu, S. Wu and B. Su, *Analyst*, 2014, **139**, 4934–4939.
27 L. Bao, Z. L. Zhang, Z. Q. Tian, L. Zhang, C. Liu, Y. Lin, B. Qi and D. W. Pang, *Adv. Mater.*, 2011, **23**, 5801–5806.
28 D. M. Hercules, *Science*, 1964, **145**, 808–809.
29 K. S. Santhana and A. J. Bard, *J. Am. Chem. Soc.*, 1965, **87**, 139–140.
30 A. W. Knight and G. M. Greenway, *Analyst*, 1994, **119**, 879–890.
31 W. Miao, *Chem. Rev.*, 2008, **108**, 2506–2553.
32 R. J. Forster, P. Bertoncello and T. E. Keyes, *Annu. Rev. Anal. Chem.*, 2009, **2**, 359–385.
33 W. J. Miao, in *Handbook of Electrochemistry*, ed. C. G. Zoski, Elsevier, Amsterdam, The Netherlands, 2007, p. 541.
34 X. Ji, W. Wang and H. Mattoussi, *Nano Today*, 2016, **11**, 98–121.
35 S. Y. Lim, W. Shen and Z. Gao, *Chem. Soc. Rev.*, 2015, **44**, 362–381.
36 Z. L. Wu, Z. X. Liu and Y. H. Yuan, *J. Mater. Chem. B*, 2017, **5**, 3794–3809.
37 L. Zheng, Y. Chi, Y. Dong, J. Lin and B. Wang, *J. Am. Chem. Soc.*, 2009, **131**, 4564.
38 J. Zhou, C. Booker, R. Li, X. Zhou, T. K. Sham, X. Sun and Z. Ding, *J. Am. Chem. Soc.*, 2007, **129**, 744–745.
39 Y. Dong, N. Zhou, X. Lin, J. Lin, Y. Chi and G. Chen, *Chem. Mater.*, 2010, **22**, 5895–5899.
40 A. Muthurasu and V. Ganesh, *Appl. Biochem. Biotechnol.*, 2014, **174**, 945–959.
41 J. Zhou, C. Booker, R. Li, X. Zhou, T. K. Sham, X. Sun and Z. Ding, *J. Am. Chem. Soc.*, 2007, **129**, 744–745.
42 A. Ananthanarayanan, X. Wang, P. Routh, B. Sana, S. Lim, D. H. Kim, K. H. Lim, J. Li and P. Chen, *Adv. Funct. Mater.*, 2014, **24**, 3021–3026.
43 L. Wang, X. Chen, Y. Lu, C. Liu and W. Yang, *Carbon*, 2015, **94**, 472–478.
44 H. Zhu, X. Wang, Y. Li, Z. Wang, F. Yang and X. Yang, *Chem. Commun.*, 2009, 5118–5120.
45 M. Shehab, S. Ebrahim and M. Soliman, *J. Lumin.*, 2017, **184**, 110–116.
46 X. Wu, F. Tian, W. Wang, J. Chen, M. Wu and J. X. Zhao, *J. Mater. Chem. C*, 2013, **1**, 4676–4684.
47 F. Arcudi, L. Dordevic and M. Prato, *Angew. Chem., Int. Ed.*, 2016, **128**, 2147–2152.
48 R. Liu, D. Wu, X. Feng and K. Mullen, *J. Am. Chem. Soc.*, 2011, **133**, 15221–15223.
49 J. J. Liu, X. L. Zhang, Z. X. Cong, Z. T. Chen, H. H. Yang and G. N. Chen, *Nanoscale*, 2013, **5**, 1810–1815.
50 L. Lin, M. Rong, S. Lu, X. Song, Y. Zhong, J. Yan, Y. Wang and X. Chen, *Nanoscale*, 2015, **7**, 1872–1878.
51 L. Wang, Y. Wang, T. Xu, H. Liao, C. Yao, Y. Liu, Z. Li, Z. Chen, D. Pan, L. Sun and M. Wu, *Nat. Commun.*, 2014, **5**, 5357–5365.
52 Q. Wang, H. Zheng, Y. Long, L. Zhang, M. Gao and W. Bai, *Carbon*, 2011, **49**, 3134–3140.
53 X. Zhai, P. Zhang, C. Liu, T. Bai, W. Li, L. Dai and W. Liu, *Chem. Commun.*, 2012, **48**, 7955–7957.
54 C. Liu, P. Zhang, F. Tian, W. Li, F. Li and W. Liu, *J. Mater. Chem.*, 2011, **21**, 13163–13167.
55 C. Liu, P. Zhang, X. Zhai, F. Tian, W. Li, J. Yang, Y. Liu, H. Wang, W. Wang and W. Liu, *Biomaterials*, 2012, **33**, 3604–3613.
56 Z. Luo, D. Yang, G. Qi, J. Shang, H. Yang, Y. Wang, L. Yuwen, T. Yu, W. Huang and L. Wang, *J. Mater. Chem. A*, 2014, **2**, 20605–20611.

57 T. Luo, L. Bu, S. Peng, Y. Zhang, Z. Zhou, G. Li and J. Huang, *Talanta*, 2019, **205**, 120117.
58 C. Lu, Q. Su and X. Yang, *Nanoscale*, 2019, **11**, 16036–16042.
59 M. Chen, C. Zhao, W. Chen, S. Weng, A. Liu, Q. Liu, Z. Zheng, J. Lin and X. Lin, *Analyst*, 2013, **138**, 7341–7346.
60 Q. Gao, J. Han and Z. Ma, *Biosens. Bioelectron.*, 2013, **49**, 323–328.
61 H. Ji, F. Zhou, J. Gu, C. Shu, K. Xi and X. Jia, *Sensors*, 2016, **16**, 630–639.
62 E. Punrat, C. Maksuk, S. Chuanuwatanakul, W. Wonsawat and O. Chailapakul, *Talanta*, 2016, **150**, 198–205.
63 J. Dong, J. Hou, J. Jiang and S. Ai, *Anal. Chim. Acta*, 2015, **885**, 92–97.
64 X. Shao, H. Gu, Z. Wang, X. Chai, Y. Tian and G. Shi, *Anal. Chem.*, 2012, **85**, 418–425.
65 L. Yang, N. Huang, Q. Lu, M. Liu, H. Li, Y. Zhang and S. Yao, *Anal. Chim. Acta*, 2016, **903**, 69–80.
66 L. Zhou, J. Huang, B. Yu and T. You, *Sci. Rep.*, 2016, **6**, 22234–22242.
67 L. Y. Zheng, Y. W. Chi, Y. Q. Dong, J. P. Lin and B. B. Wang, *J. Am. Chem. Soc.*, 2009, **131**, 4564–4565.
68 J. Zhou, C. Booker, R. Li, X. Sun, T. K. Sham and Z. Ding, *Chem. Phys. Lett.*, 2010, **493**, 296–298.
69 Y. Dong, C. Chen, J. Lin, N. Zhou, Y. Chi and G. Chen, *Carbon*, 2013, **56**, 12–17.
70 Y. M. Long, L. Bao, Y. Peng, Z. L. Zhang and D. W. Pang, *Carbon*, 2018, **129**, 168–174.
71 R. Zhang, J. R. Adsetts, Y. Nie, X. Sun and Z. Ding, *Carbon*, 2018, **129**, 45–53.
72 X. Wang, M. Zhang, X. Huo, W. Zhao, B. Kang, J. J. Xu and H. Chen, *Nanoscale Adv.*, 2019, **1**, 1965–1969.
73 M. Wang, R. Sun, Q. Wang, L. Chen, L. Hou, Y. Chi, C. H. Lu, F. Fu and Y. Dong, *Chemistry*, 2018, **24**, 4250–4254.
74 Y. Qin, N. Liu, H. Li, Y. Sun, L. Hu, S. Zhao, D. Han, Y. Liu, Z. Kang and L. Niu, *J. Phys. Chem. C*, 2017, **121**, 27546–27554.
75 Y. Y. Lu, N. L. Li, L. P. Jia, R. N. Ma, W. L. Jia, X. Q. Tao, H. Cui and H. S. Wang, *J. Electroanal. Chem.*, 2016, **781**, 114–119.
76 Y. Yan, Q. Liu, H. Mao and K. Wang, *J. Electroanal. Chem.*, 2016, **775**, 1–7.
77 Y. Chen, Y. Dong, H. Wu, C. Chen, Y. Chi and G. Chen, *Electrochim. Acta*, 2015, **151**, 552–557.
78 Z. X. Wang, C. L. Zheng, Q. L. Li and S. N. Ding, *Analyst*, 2014, **139**, 1751–1755.
79 P. J. Zhang, Z. J. Xue, D. Luo, W. Yu, Z. H. Guo and T. Wang, *Anal. Chem.*, 2014, **86**, 5620–5623.
80 Y. Xu, M. Wu, X. Z. Feng, X. B. Yin, X. W. He and Y. K. Zhang, *Chemistry*, 2013, **19**, 6282–6288.
81 Y. Dong, W. Tian, S. Ren, R. Dai, Y. Chi and G. Chen, *ACS Appl. Mater. Interfaces*, 2014, **6**, 1646–1651.
82 L. L. Li, J. Ji, R. Fei, C. Z. Wang, Q. Lu, J. R. Zhang, L. P. Jiang and J. J. Zhu, *Adv. Funct. Mater.*, 2012, **22**, 2971–2979.
83 H. Hai, F. Yang and J. Li, *Microchim. Acta*, 2014, **181**, 893–901.
84 M. Wang, Y. Sun and M. Yang, *Chem. Lett.*, 2018, **47**, 44–47.
85 Y. Tang, J. Li, Q. Guo and G. Nie, *Sens. Actuators, B*, 2019, **282**, 824–830.
86 N. Tassali, N. Kotera, C. Boutin, E. Léonce, Y. Boulard, B. Rousseau, E. Dubost, F. Taran, T. Brotin, J.-P. Dutasta and P. Berthault, *Anal. Chem.*, 2014, **86**, 1783–1788.
87 K. A. Morales, M. Lasagna, A. V. Gribenko, Y. Yoon, G. D. Reinhart, J. C. Lee, W. Cho, P. Li and T. I. Igumenova, *J. Am. Chem. Soc.*, 2011, **133**, 10599–10611.
88 C. Xiong, W. Liang, H. Wang, Y. Zheng, Y. Zhuo, Y. Chai and R. Yuan, *Chem. Commun.*, 2016, **52**, 5589–5592.
89 S. Li, J. Li, X. Ma, C. Pang, G. Yin and J. Luo, *Biosens. Bioelectron.*, 2019, **139**, 111321.
90 H. Chen, W. Li, Q. Wang, X. Jin, Z. Nie and S. Yao, *Electrochim. Acta*, 2016, **214**, 94–102.
91 Z. Lin, X. Li and H. B. Kraatz, *Anal. Chem.*, 2011, **83**, 6896–6901.
92 A. W. Martinez, S. T. Phillips, M. J. Butte and G. M. Whitesides, *Angew. Chem., Int. Ed.*, 2007, **46**, 1318–1320.
93 S. Su, R. Nutiu, C. D. M. Filipe, Y. Li and R. Pelton, *Langmuir*, 2007, **23**, 1300–1302.
94 Z. Nie, F. Deiss, X. Liu, O. Akbulut and G. M. Whitesides, *Lab Chip*, 2010, **10**, 3163–3169.
95 M. Zhang, L. Ge, S. Ge, M. Yan, J. Yu, J. Huang and S. Liu, *Biosens. Bioelectron.*, 2013, **41**, 544–550.
96 F. Salehnia, M. Hosseini and M. R. Ganjali, *Anal. Methods*, 2018, **10**, 508–514.
97 S. Zhu, X. Lin, P. Ran, F. Mo, Q. Xia and Y. Fu, *Microchim. Acta*, 2017, **184**, 4679–4684.
98 Z. Liu, X. Zhang, L. Cui, K. Wang and H. Zhan, *Sens. Actuators, B*, 2017, **248**, 402–410.
99 Y. Yan, H. Li, Q. Wang, H. Mao and W. Kun, *J. Mater. Chem. C*, 2017, **5**, 6092–6100.
100 Y. Yan, Q. Liu, X. Dong, N. Hao, S. Chen, T. You, H. Mao and K. Wang, *Microchim. Acta*, 2016, **183**, 1591–1599.
101 W. J. Niu, R. H. Zhu, S. Cosnier, X. J. Zhang and D. Shan, *Anal. Chem.*, 2015, **87**, 11150–11156.
102 Q. Li, W. Tang, Y. Wang, J. Di, J. Yang and Y. Wu, *J. Solid State Electrochem.*, 2015, **19**, 2973–2980.
103 H. Chen, W. Li, P. Zhao, Z. Nie and S. Yao, *Electrochim. Acta*, 2015, **178**, 407–413.
104 X. Du, D. Jiang, Q. Liu, G. Zhu, H. Mao and K. Wang, *Analyst*, 2015, **140**, 1253–1259.
105 T. T. Zhang, H. M. Zhao, X. F. Fan, S. Chen and X. Quan, *Talanta*, 2015, **131**, 379–385.
106 J. Lu, M. Yan, L. Ge, S. Ge, S. Wang, J. Yan and J. Yu, *Biosens. Bioelectron.*, 2013, **47**, 271–277.
107 J. Li, N. Wang, T. T. Tran, C. Huang, L. Chen, L. Yuan, L. Zhou, R. Shen and Q. Cai, *Analyst*, 2013, **138**, 2038–2043.
108 S. Yang, J. Liang, S. Luo, C. Liu and Y. Tang, *Anal. Chem.*, 2013, **85**, 7720–7725.
109 Q. Liu, K. Wang, J. Huan, G. Zhu, J. Qian, H. Mao and J. Cai, *Analyst*, 2014, **139**, 2912–2918.
110 K. Tian, F. Nie, K. Luo, X. Zheng and J. Zheng, *J. Electroanal. Chem.*, 2017, **801**, 162–170.
111 P. Ran, J. Song, F. Mo, J. Wu, P. Liu and Y. Fu, *Microchim. Acta*, 2019, **186**, 276.

112 X. L. Zhang, X. Li, X. T. Li, Y. Gao, F. Feng and G. J. Yang, *Sens. Actuators, B*, 2019, **282**, 927–935.
113 H. Yuan, D. Li, Y. Liu, X. Xu and C. Xiong, *Analyst*, 2015, **140**, 1428–1431.
114 Z. Yu, F. Wang, X. Lin, C. Wang, Y. Fu, X. Wang, Y. Zhao and G. Li, *J. Solid State Chem.*, 2015, **232**, 96–101.
115 X. Chen, X. Cheng and J. J. Gooding, *Anal. Chem.*, 2012, **84**, 8557–8563.
116 S. Chen, X. Chen, T. Xia and Q. Ma, *Biosens. Bioelectron.*, 2016, **85**, 903–908.
117 C. Zhou, Y. Chen, X. You, Y. Dong and Y. Chi, *ChemElectroChem*, 2017, **4**, 1783–1789.
118 D. Wang, Y. Liang, Y. Su, Q. Shang and C. Zhang, *Biosens. Bioelectron.*, 2019, **130**, 55–64.
119 Y. Wu, Y. Chen, S. Zhang, L. Zhang and J. Gong, *Anal. Chim. Acta*, 2019, **1073**, 45–53.
120 Y. Hu, L. Su, S. Wang, Z. Guo, Y. Hu and H. Xie, *Microchim. Acta*, 2019, **186**, 512.
121 H. Chen, X. Liu, C. Yin, W. Li, X. Qin and C. Chen, *Analyst*, 2019, **144**, 5215–5222.
122 S. Li, J. Li, X. Ma, C. Liu, C. Pang and J. Luo, *Microchem. J.*, 2019, **148**, 397–403.
123 S. Li, C. Liu, G. Yin, Q. Zhang, J. Luo and N. Wu, *Biosens. Bioelectron.*, 2017, **91**, 687–691.
124 Y. Yang, G. Fang, X. Wang, F. Zhang, J. Liu, W. Zheng and S. Wang, *Electrochim. Acta*, 2017, **228**, 107–113.
125 J. Zhou, T. Han, H. Ma, T. Yan, X. Pang, Y. Li and Q. Wei, *Anal. Chim. Acta*, 2015, **889**, 82–89.
126 K. Tian, D. Li, T. Tang, F. Nie, Y. Zhou, J. Du and J. Zheng, *Talanta*, 2018, **185**, 446–452.
127 S. Tombelli, M. Minunni and M. Mascini, *Biosens. Bioelectron.*, 2005, **20**, 2424–2434.
128 S. Li, X. Wu, C. Liu, G. Yin, J. Luo and Z. Xu, *Anal. Chim. Acta*, 2016, **941**, 94–100.
129 Y. Xu, J. Liu, J. Zhang, X. Zong, X. Jia, D. Li and E. Wang, *Nanoscale*, 2015, **7**, 9421–9426.
130 B. P. Qi, X. Zhang, B. B. Shang, D. Xiang, W. Qu and S. Zhang, *Carbon*, 2017, **121**, 72–78.
131 S. Carrara, F. Arcudi, M. Prato and L. De Cola, *Angew. Chem., Int. Ed.*, 2017, **129**, 4835–4839.
132 Y. M. Long, L. Bao, J. Y. Zhao, Z. L. Zhang and D. W. Pang, *Anal. Chem.*, 2014, **86**, 7224–7228.
133 L. Li, B. Yu, X. Zhang and T. You, *Anal. Chim. Acta*, 2015, **895**, 104–111.
134 Z. Xu, J. Yu and G. Liu, *Sens. Actuators, B*, 2013, **181**, 209–214.
135 L. Luo, S. Ma, L. Li, X. Liu, J. Zhang, X. Li, D. Liu and T. You, *Food Chem.*, 2019, **292**, 98–105.
136 L. Luo, L. Li, X. Xu, D. Liu, J. Li, K. Wang and T. You, *RSC Adv.*, 2017, **7**, 50634–50642.
137 G. W. Muna, V. Quaiserová-Mocko and G. M. Swain, *Anal. Chem.*, 2005, **77**, 6542–6548.
138 L. Li, D. Liu, H. Mao and T. You, *Biosens. Bioelectron.*, 2017, **89**, 489–495.
139 Y. Nie, Y. Liu, Q. Zhang, X. Su and Q. Ma, *Biosens. Bioelectron.*, 2019, **138**, 111318.
140 M. Zhang, W. Dai, M. Yan, S. Ge, J. Yu, X. Song and W. Xu, *Analyst*, 2012, **137**, 2112–2118.
141 H. Yang, W. Liu, C. Ma, Y. Zhang, X. Wang, J. Yu and X. Song, *Electrochim. Acta*, 2014, **123**, 470–476.
142 W. Deng, F. Liu, S. Ge, J. Yu, M. Yan and X. Song, *Analyst*, 2014, **139**, 1713–1720.
143 W. Liu, C. Ma, H. Yang, Y. Zhang, M. Yan, S. Ge, J. Yu and X. Song, *Microchim. Acta*, 2014, **181**, 1415–1422.
144 S. Li, J. Luo, X. Yang, Y. Wan and C. Liu, *Sens. Actuators, B*, 2014, **197**, 43–49.
145 L. Wu, M. Li, M. Zhang, M. Yan, S. Ge and J. Yu, *Sens. Actuators, B*, 2013, **186**, 761–767.
146 F. Du, H. Zhang, X. Tan, C. Ai, M. Li, J. Yan, M. Liu, Y. Wu, D. Feng, S. Liu and H. Han, *J. Solid State Electrochem.*, 2019, **23**, 2579–2588.
147 Y. N. Khonsari and S. Sun, *Mater. Sci. Eng., C*, 2019, **96**, 146–152.
148 Y. N. Khonsari and S. Sun, *Microchim. Acta*, 2018, **185**, 430.
149 C. Tian, L. Wang, F. Luan and X. Zhuang, *Talanta*, 2019, **191**, 103–108.
150 Y. Dong, H. Wu, P. Shang, X. Zeng and Y. Chi, *Nanoscale*, 2015, **7**, 16366–16371.
151 W. Zhu, M. Saddam Khan, W. Cao, X. Sun, H. Ma, Y. Zhang and Q. Wei, *Biosens. Bioelectron.*, 2018, **99**, 346–352.
152 R. P. Liang, W. B. Qiu, H. F. Zhao, C. Y. Xiang and J. D. Qiu, *Anal. Chim. Acta*, 2016, **904**, 58–64.
153 Y. Dong, Y. Peng, J. Wang and C. Wang, *Microchim. Acta*, 2017, **184**, 2089–2095.
154 X. L. Cai, B. Zheng, Y. Zhou, M. R. Younis, F. B. Wang, W. M. Zhang, Y. G. Zhou and X. H. Xia, *Chem. Sci.*, 2018, **9**, 6080–6084.
155 J. Liu, X. He, K. Wang, D. He, Y. Wang, Y. Mao, H. Shi and L. Wen, *Biosens. Bioelectron.*, 2015, **70**, 54–60.
156 N. L. Li, L. P. Jia, R. N. Ma, W. L. Jia, Y. Y. Lu, S. S. Shi and H. S. Wang, *Biosens. Bioelectron.*, 2017, **89**, 453–460.
157 G. Nie, Y. Wang, Y. Tang, D. Zhao and Q. Guo, *Biosens. Bioelectron.*, 2018, **101**, 123–128.
158 D. Qin, X. Jiang, G. Mo, J. Feng, C. Yu and B. Deng, *ACS Sens.*, 2019, **4**, 504–512.
159 F. Zuo, C. Zhang, H. Zhang, X. Tan, S. Chen and R. Yuan, *Electrochim. Acta*, 2019, **294**, 76–83.
160 L. Li, W. Li, C. Ma, H. Yang, S. Ge and J. Yu, *Sens. Actuators, B*, 2014, **202**, 314–322.
161 L. L. Xu, W. Zhang, L. Shang, R. N. Ma, L. P. Jia, W. L. Jia, H. S. Wang and L. Niu, *Biosens. Bioelectron.*, 2018, **103**, 6–11.
162 H. F. Zhao, R. P. Liang, J. W. Wang and J. D. Qiu, *Chem. Commun.*, 2015, **51**, 12669–12672.
163 G. Aragay, H. Montón, J. Pons, M. Font-Bardía and A. Merkoçi, *J. Mater. Chem.*, 2012, **22**, 5978–5983.
164 R. F. Carvalhal, M. Simão Kfouri, M. H. de Oliveira Piazetta, A. L. Gobbi and L. T. Kubota, *Anal. Chem.*, 2010, **82**, 1162–1165.
165 S. Wang, L. Ge, X. Song, J. Yu, S. Ge, J. Huang and F. Zeng, *Biosens. Bioelectron.*, 2012, **31**, 212–218.
166 L. Zhang, L. Li, C. Ma, S. Ge, M. Yan and C. Bian, *Sens. Actuators, B*, 2015, **221**, 799–806.

167 G. Mo, X. He, C. Zhou, D. Ya, J. Feng, C. Yu and B. Deng, *Biosens. Bioelectron.*, 2019, **126**, 558–564.
168 L. Wu, C. Ma, X. Zheng, H. Liu and J. Yu, *Biosens. Bioelectron.*, 2015, **68**, 413–420.
169 D. Wang, N. Gan, H. Zhang, T. Li, L. Qiao, Y. Cao, X. Su and S. Jiang, *Biosens. Bioelectron.*, 2015, **65**, 78–82.
170 B. Zhou, M. Zhu, Y. Qiu and P. Yang, *ACS Appl. Mater. Interfaces*, 2017, **9**, 18493–18500.
171 M. S. Wu, Z. Liu, H. W. Shi, H. Y. Chen and J. J. Xu, *Anal. Chem.*, 2015, **87**, 530–537.
172 B. Zhou, M. Zhu, Y. Hao and P. Yang, *ACS Appl. Mater. Interfaces*, 2017, **9**, 30536–30542.
173 S. Wang, L. Ge, Y. Zhang, X. Song, N. Li, S. Ge and J. Yu, *Lab Chip*, 2012, **12**, 4489–4498.
174 W. G. Kaelin, *Oncogene*, 1999, **18**, 7701–7705.
175 Q. Lu, W. Wei, Z. Zhou, Z. Zhou, Y. Zhang and S. Liu, *Analyst*, 2014, **139**, 2404–2410.
176 I. J. Holt, A. E. Harding and J. A. Morgan Hughes, *Nature*, 1988, **331**, 717–719.
177 K. L. Liaw, A. Hildesheim, R. D. Burk, P. Gravitt, S. Wacholder, M. M. Manos, D. R. Scott, M. E. Sherman, R. J. Kurman, A. G. Glass, S. M. Anderson and M. Schiffman, *J. Infect. Dis.*, 2001, **183**, 8–15.
178 H. Zhang, F. Li, B. Dever, X. F. Li and X. C. Le, *Chem. Rev.*, 2013, **113**, 2812–2841.
179 W. Zhou, X. Gao, D. Liu and X. Chen, *Chem. Rev.*, 2015, **115**, 10575–10636.
180 M. Yan, M. Zhang, S. Ge, J. Yu, M. Li, J. Huang and S. Liu, *Analyst*, 2012, **137**, 3314–3320.
181 R. M. Dirks and N. A. Pierce, *Proc. Natl. Acad. Sci. U. S. A.*, 2004, **101**, 15275.
182 P. Yin, H. M. T. Choi, C. R. Calvert and N. A. Pierce, *Nature*, 2008, **451**, 318.
183 J. Y. Kishi, T. E. Schaus, N. Gopalkrishnan, F. Xuan and P. Yin, *Nat. Chem.*, 2017, **10**, 155.
184 L. P. Qiu, Z. S. Wu, G. L. Shen and R. Q. Yu, *Anal. Chem.*, 2011, **83**, 3050–3057.
185 A. Csordas, A. E. Gerdon, J. D. Adams, J. Qian, S. S. Oh, Y. Xiao and H. T. Soh, *Angew. Chem., Int. Ed.*, 2010, **49**, 355–358.
186 G. Jie, J. Yuan and J. Zhang, *Biosens. Bioelectron.*, 2012, **31**, 69–76.
187 C. Zhao, L. Wu, J. Ren and X. Qu, *Chem. Commun.*, 2011, **47**, 5461–5463.
188 G. Jie, Q. Zhou and G. Jie, *Talanta*, 2019, **194**, 658–663.
189 J. Lou, S. Liu, W. Tu and Z. Dai, *Anal. Chem.*, 2015, **87**, 1145–1151.
190 X. Wang, L. Liu, Z. Wang and Z. Dai, *J. Electroanal. Chem.*, 2016, **781**, 351–355.
191 P. Zhang, Y. Zhuo, Y. Chang, R. Yuan and Y. Chai, *Anal. Chem.*, 2015, **87**, 10385–10391.
192 T. Zhang, H. Zhao, G. Fan, Y. Li, L. Li and X. Quan, *Electrochim. Acta*, 2016, **190**, 1150–1158.
193 Q. Liu, C. Ma, X. P. Liu, Y. P. Wei, C. J. Mao and J. J. Zhu, *Biosens. Bioelectron.*, 2017, **92**, 273–279.
194 R. Zhang, A. Chen, Y. Yu, Y. Chai, Y. Zhuo and R. Yuan, *Microchim. Acta*, 2018, **185**, 432.
195 F. Liu, G. Xiang, D. Jiang, L. Zhang, X. Chen, L. Liu, F. Luo, Y. Li, C. Liu and X. Pu, *Biosens. Bioelectron.*, 2015, **74**, 214–221.
196 J. J. Li, L. Shang, L. P. Jia, R. N. Ma, W. Zhang, W. L. Jia, H. S. Wang and K. H. Xu, *J. Electroanal. Chem.*, 2018, **824**, 114–120.
197 M. Su, H. Liu, L. Ge, Y. Wang, S. Ge, J. Yu and M. Yan, *Electrochim. Acta*, 2014, **146**, 262–269.
198 M. Zhang, H. Liu, L. Chen, M. Yan, L. Ge, S. Ge and J. Yu, *Biosens. Bioelectron.*, 2013, **49**, 79–85.
199 L. Wu, J. Wang, J. Ren, W. Li and X. Qu, *Chem. Commun.*, 2013, **49**, 5675–5677.
200 F. Liu, S. Ge, M. Su, X. Song, M. Yan and J. Yu, *Biosens. Bioelectron.*, 2015, **71**, 286–293.
201 Y. Qiu, B. Zhou, X. Yang, D. Long, Y. Hao and P. Yang, *ACS Appl. Mater. Interfaces*, 2017, **9**, 16848–16856.
202 D. Long, C. Chen, C. Cui, Z. Yao and P. Yang, *Nanoscale*, 2018, **10**, 18597–18605.
203 L. Wu, Y. Zhang, Y. Wang, S. Ge, H. Liu, M. Yan and J. Yu, *Microchim. Acta*, 2016, **183**, 1873–1880.
204 D. Long, Y. Shang, Y. Qiu, B. Zhou and P. Yang, *Biosens. Bioelectron.*, 2018, **102**, 553–559.
205 H. Yang, Y. Zhang, L. Li, L. Zhang, F. Lan and J. Yu, *Anal. Chem.*, 2017, **89**, 7511–7519.
206 S. Li, J. Liu, Z. Chen, Y. Lu, S. S. Low, L. Zhu, C. Cheng, Y. He, Q. Chen, B. Su and Q. Liu, *Sens. Actuators, B*, 2019, **297**, 126811.
207 Y. Zhang, C. Tan, R. Fei, X. Liu, Y. Zhou, J. Chen, H. Chen, R. Zhou and Y. Hu, *Anal. Chem.*, 2014, **86**, 1115–1122.
208 R. R. Hu, Z. Z. Yin, Y. B. Zeng, J. Zhang, H. Q. Liu, Y. Shao, S. B. Ren and L. Li, *Biosens. Bioelectron.*, 2016, **78**, 31–36.
209 S. Chen, X. Chen, L. Zhang, J. Gao and Q. Ma, *ACS Appl. Mater. Interfaces*, 2017, **9**, 5430–5436.
210 C. Ma, W. Wu, Y. Peng, M. X. Wang, G. Chen, Z. Chen and J. J. Zhu, *Anal. Chem.*, 2018, **90**, 1334–1339.
211 C. Ma, W. Wu, L. Li, S. Wu, J. Zhang, Z. Chen and J. J. Zhu, *Chem. Sci.*, 2018, **9**, 6167–6175.
212 G. Liu, B. K. Jin, C. Ma, Z. Chen and J. J. Zhu, *Anal. Chem.*, 2019, **91**, 6363–6370.